Muscle representation in the macaque motor cortex: An anatomical perspective

Jean-Alban Rathelot*† and Peter L. Strick*†‡§¶||

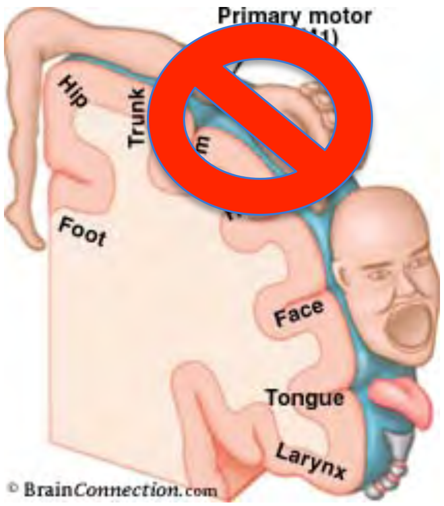

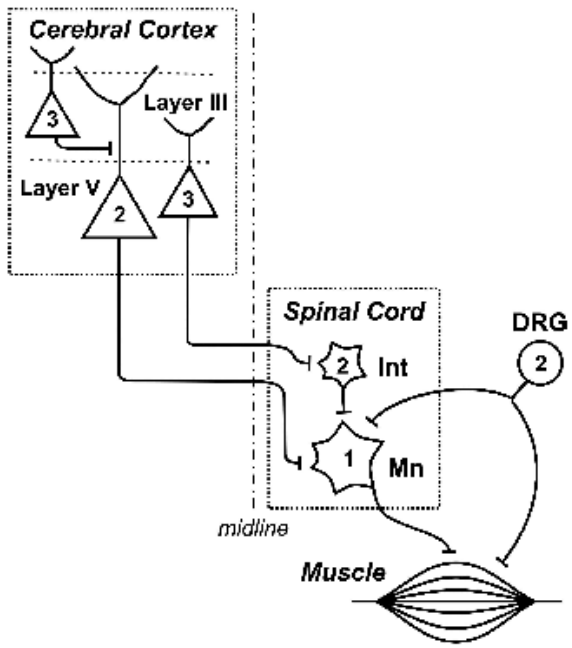

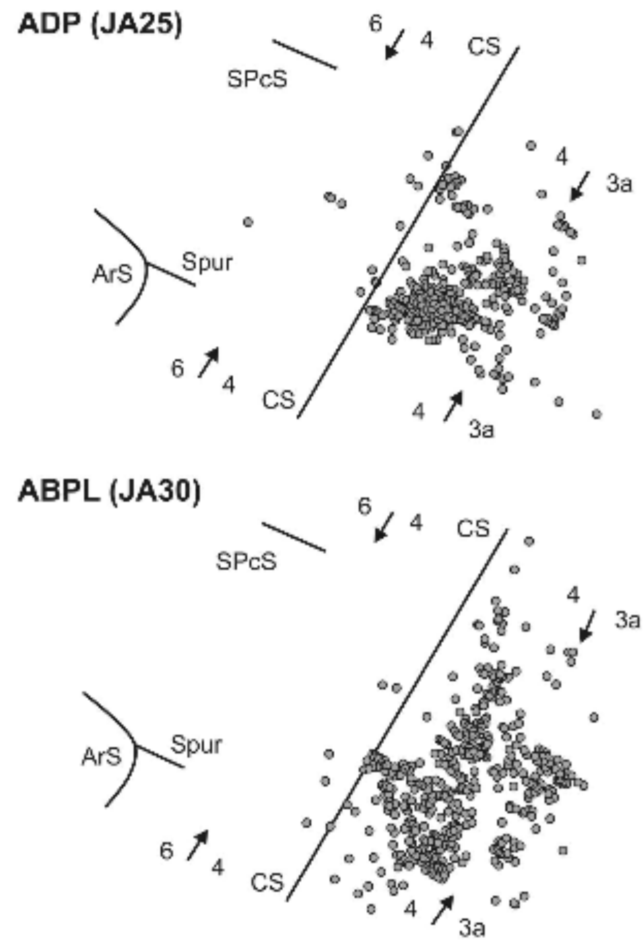

Combinations of muscle synergies in the construction of a natural motor behavior

Andrea d'Avella[1,2], Philippe Saltiel[1] and Emilio Bizzi[1]

nature *neuroscience* • volume 6 no 3 • march 2003

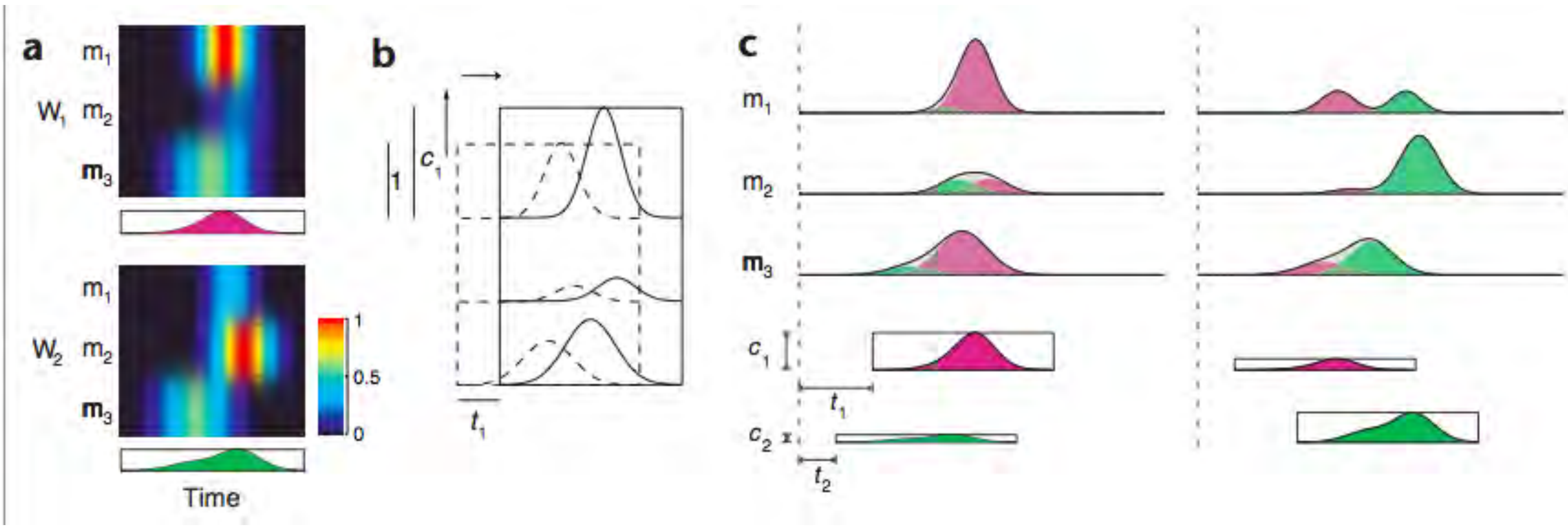

Rapid formation and selective stabilization of synapses for enduring motor memories

Vol 462 | 17 December 2009 | doi:10.1038/nature08389

Tonghui Xu[1]*, Xinzhu Yu[1]*, Andrew J. Perlik[1], Willie F. Tobin[1], Jonathan A. Zweig[1], Kelly Tennant[2], Theresa Jones[2] & Yi Zuo[1]

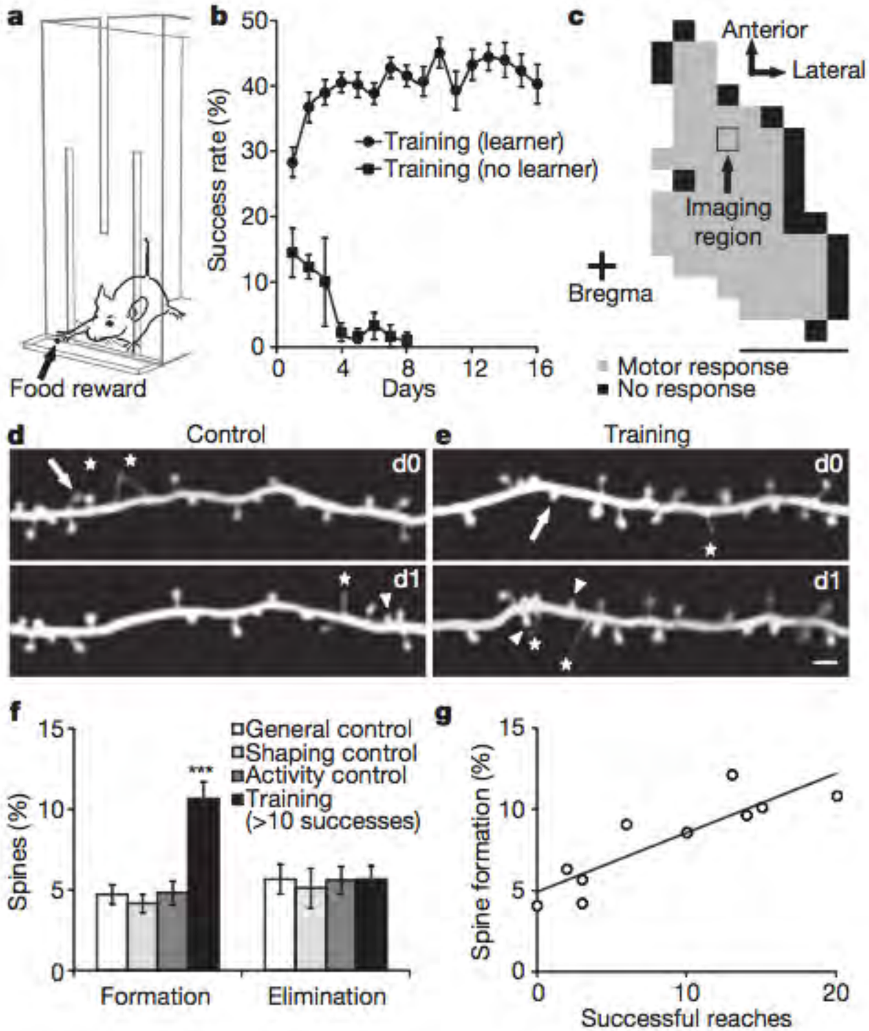

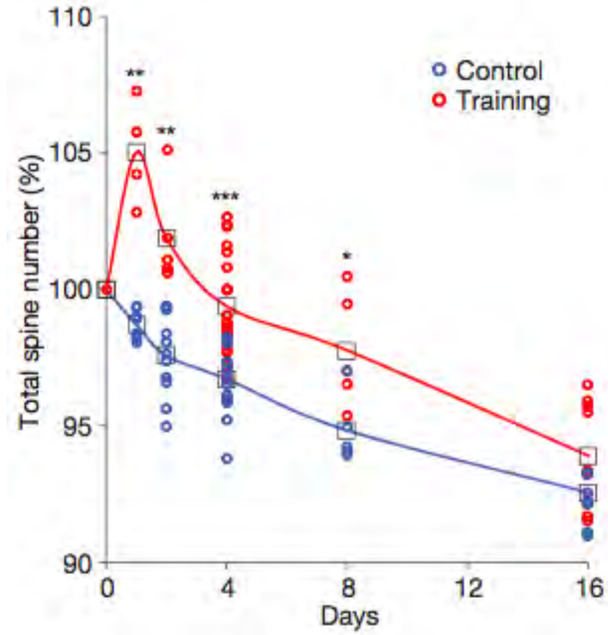

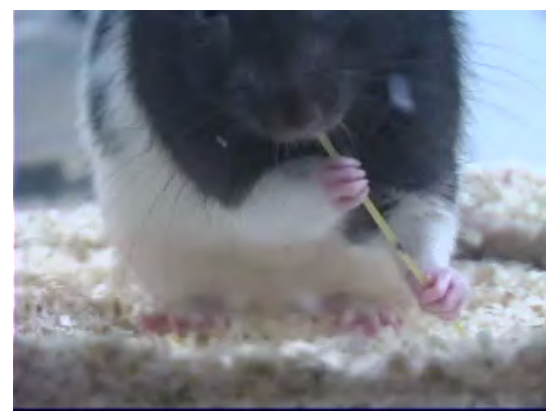

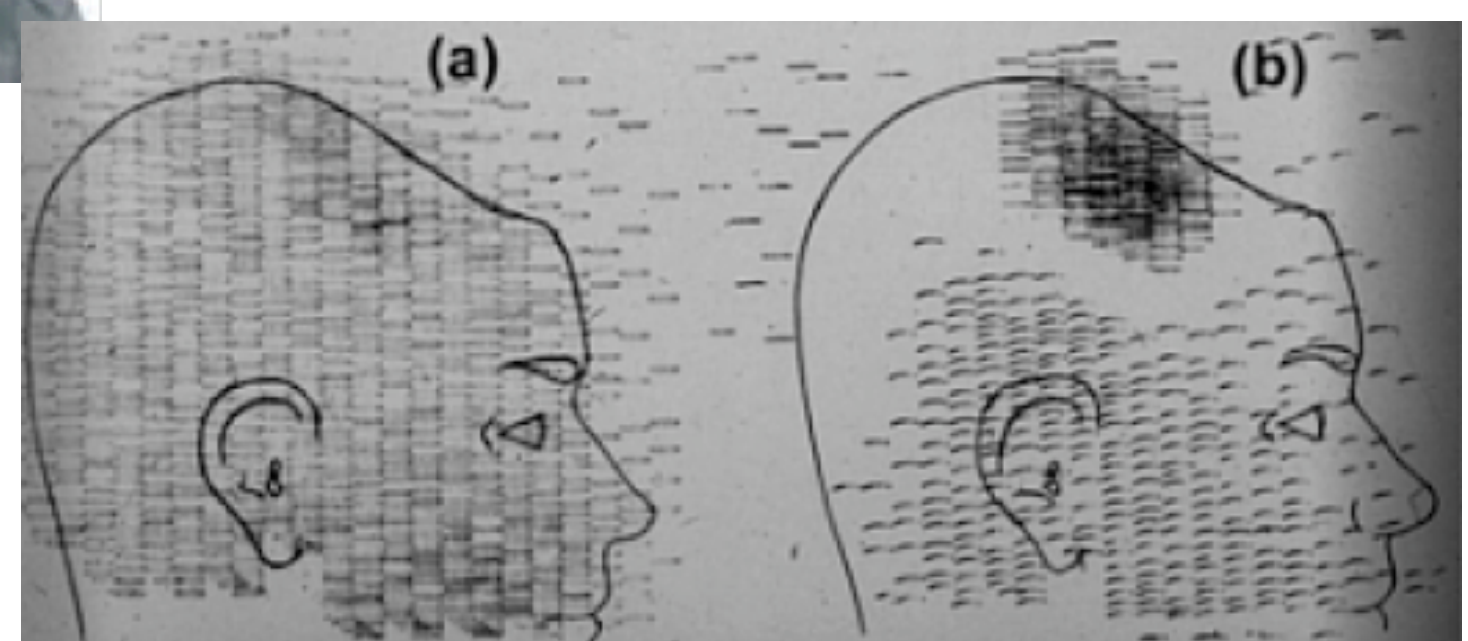
(a)
(b)

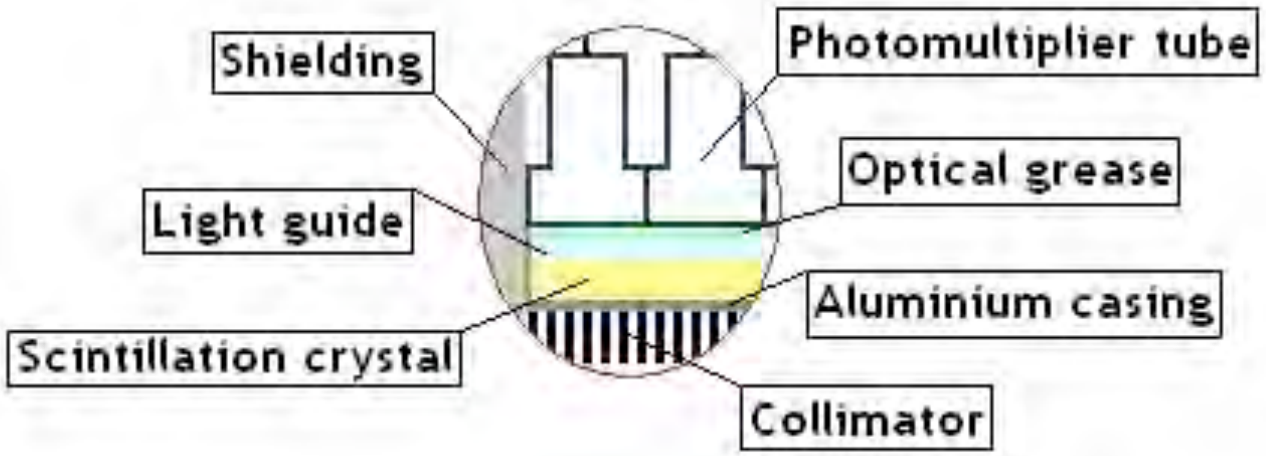

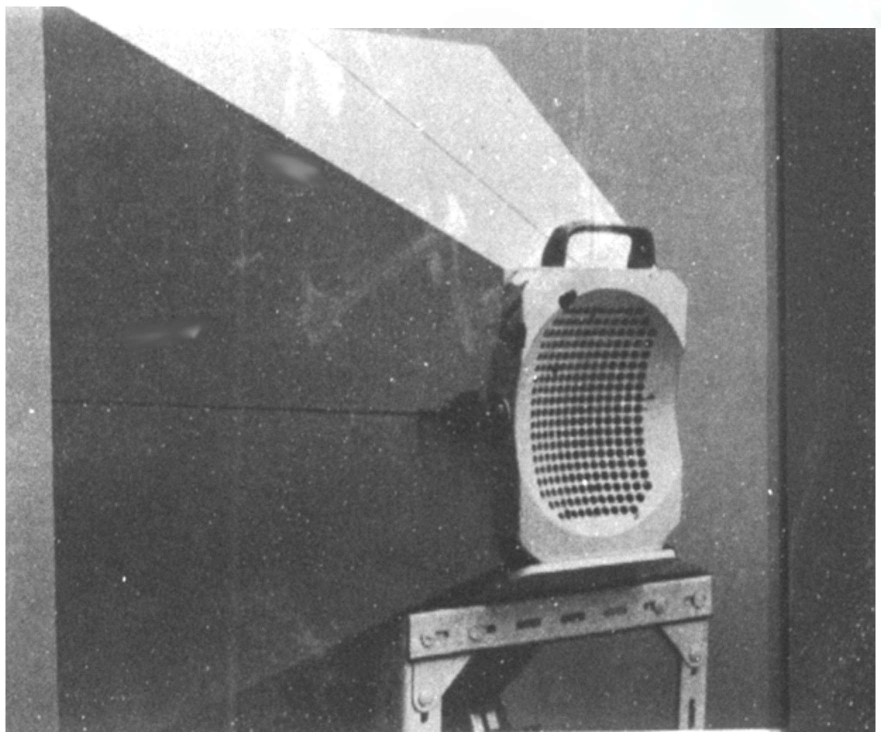

Planar Brain Imaging with Radionuclides: 1970’s

Moving fingers

Speaking

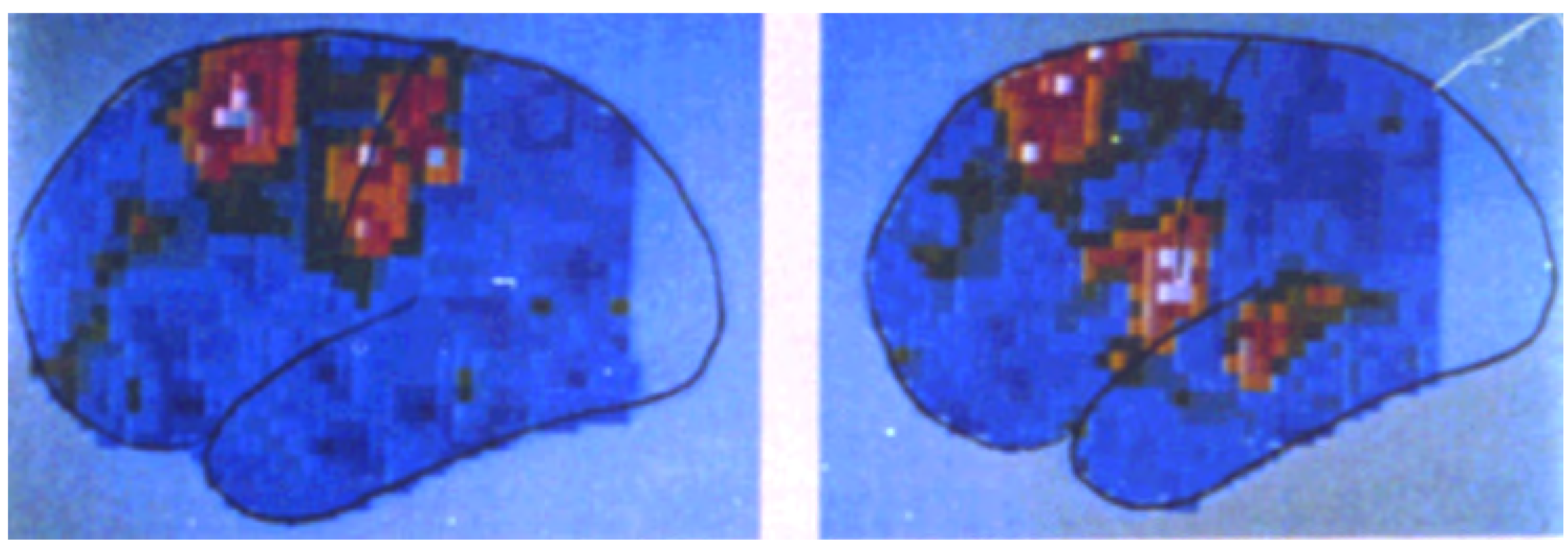

Local cerebral glucose utilization and blood flow during metabolic acidosis

W. KUSCHINSKY, S. SUDA, AND L. SOKOLOFF
Laboratory of Cerebral Metabolism, National Institute of Mental Health, Bethesda, Maryland 20205

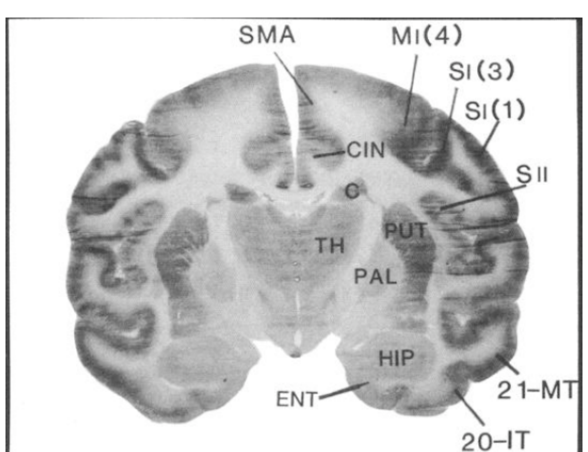

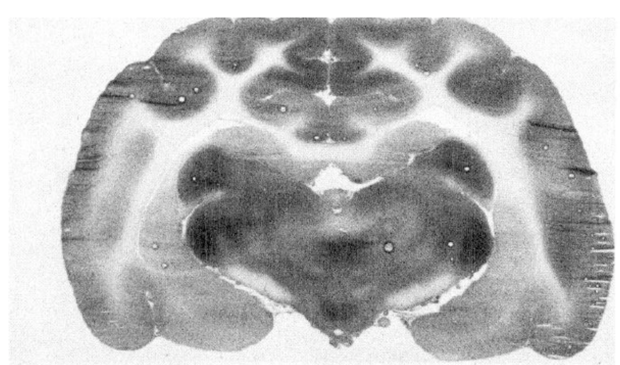

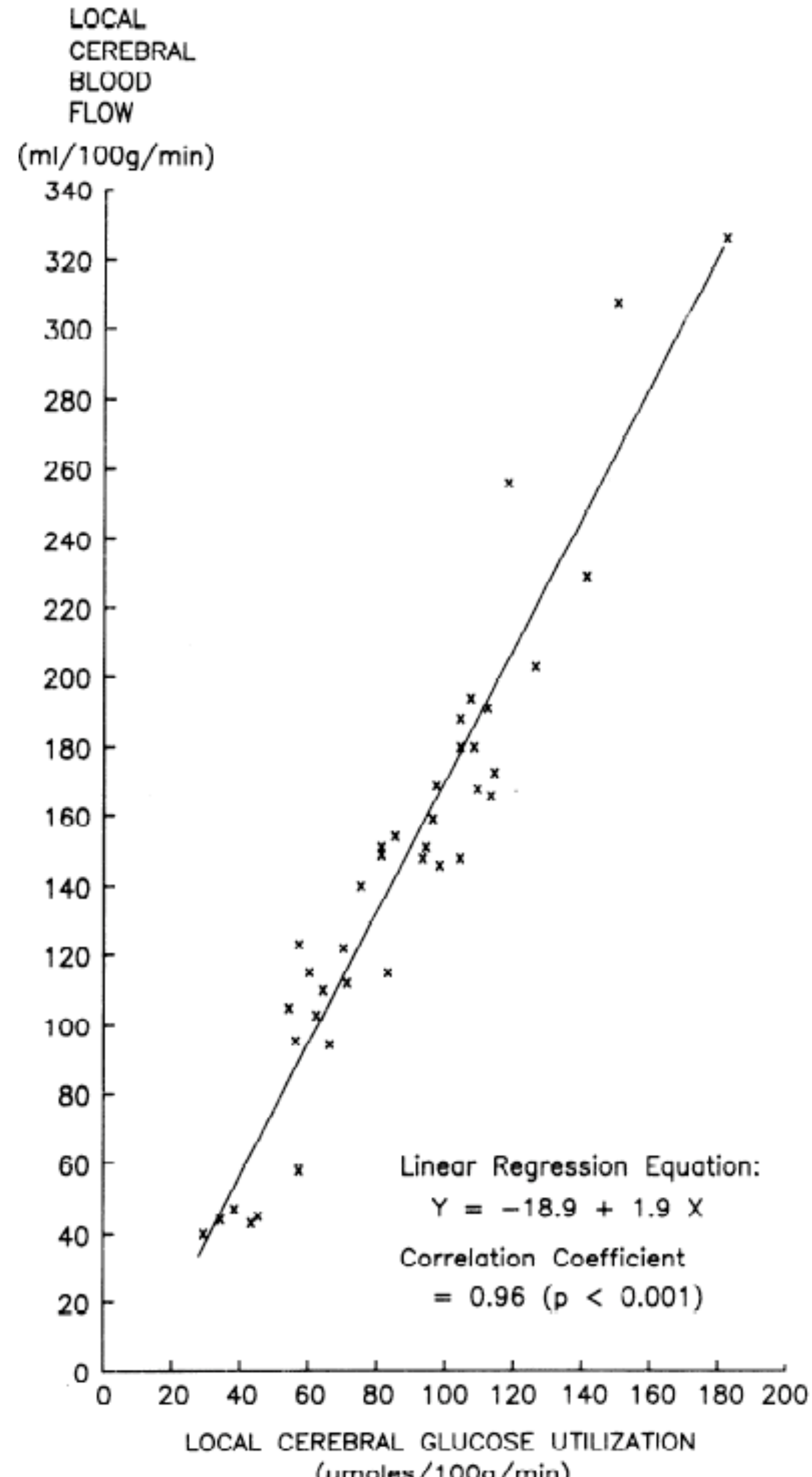

How do you increase spatial sampling?

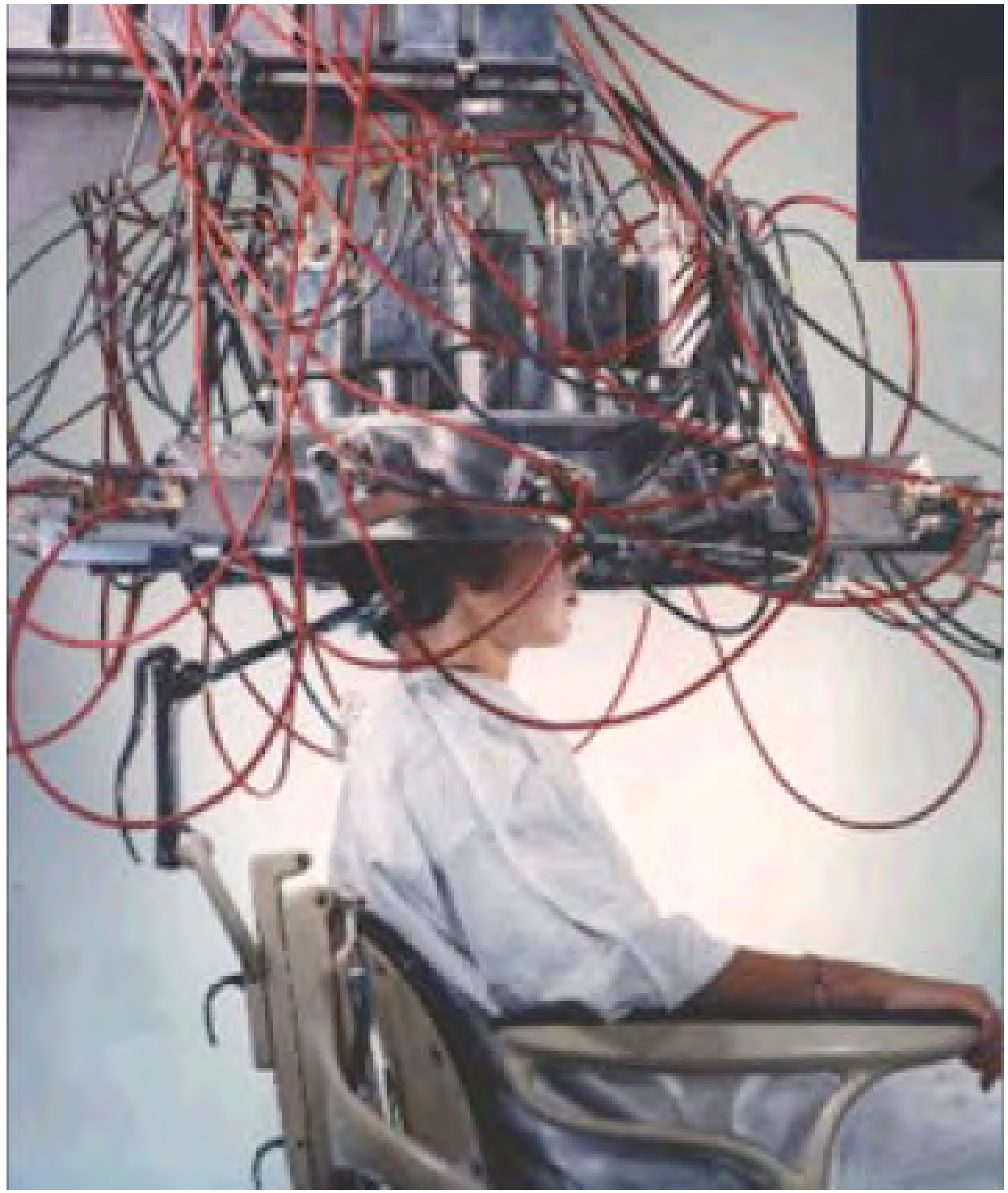

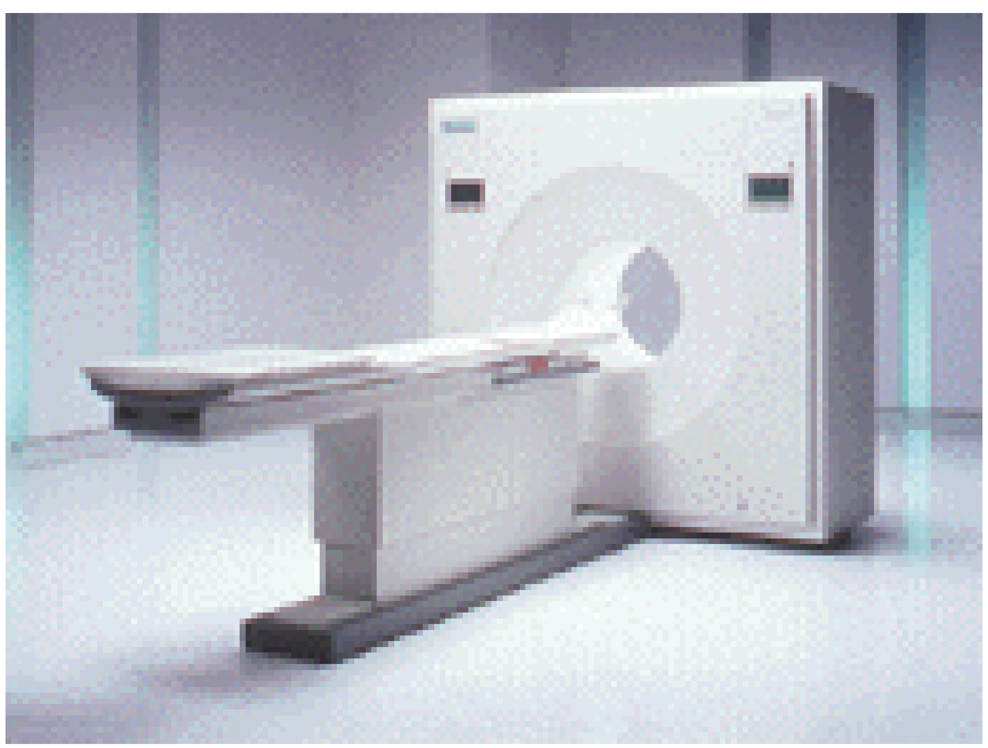

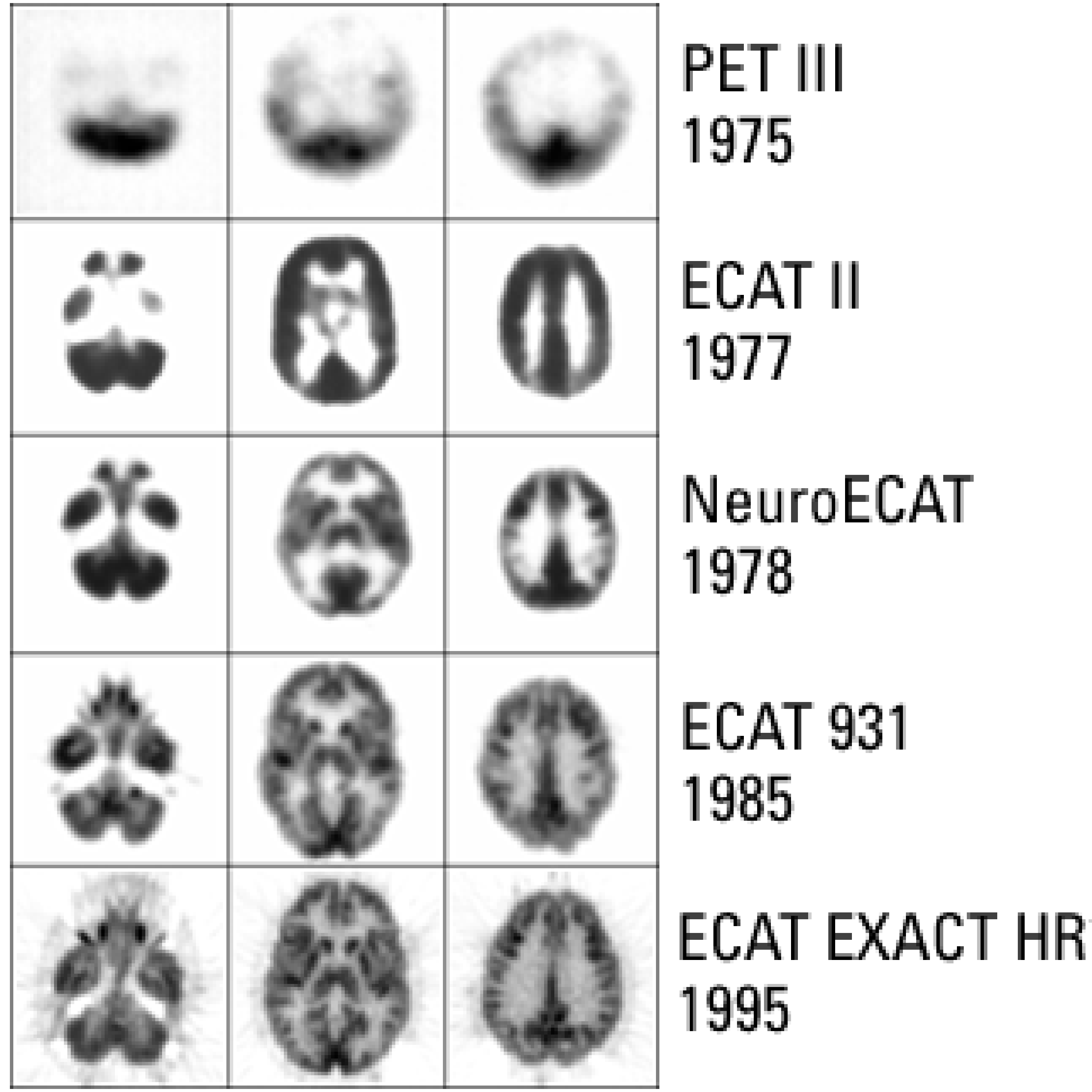
PET III
1975
ECAT II
1977
NeuroECAT
1978
ECAT 931
1985
ECAT EXACT HR$^+$
1995

Cerebral Blood Flow

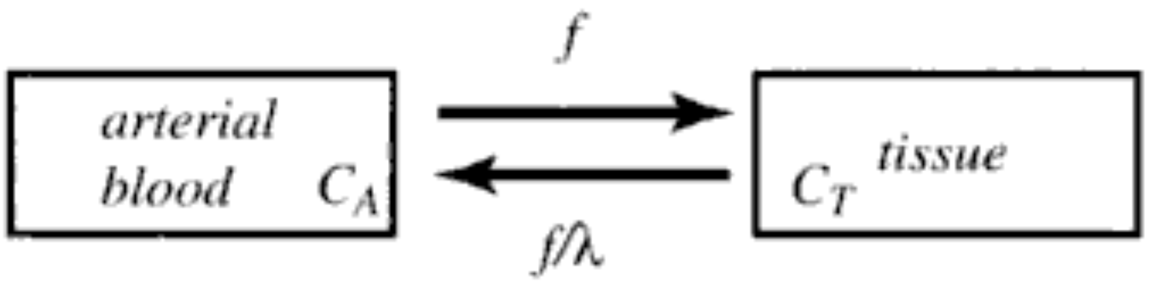

$$\frac{dC_T}{dt} = f\,C_A - \frac{f}{\lambda}\,C_T$$

$$C(t) = f\int_0^t C_A(t')\,e^{-(t-t')f/\lambda}\,dt'$$

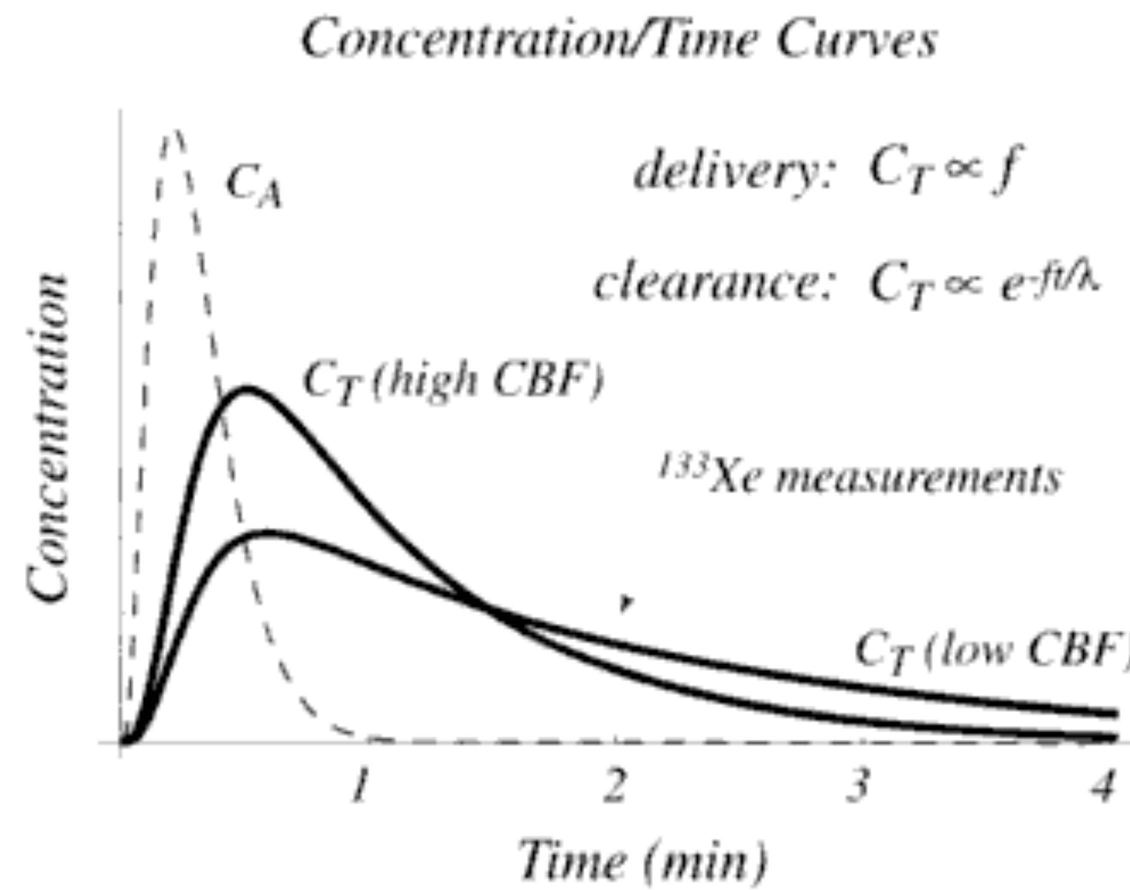

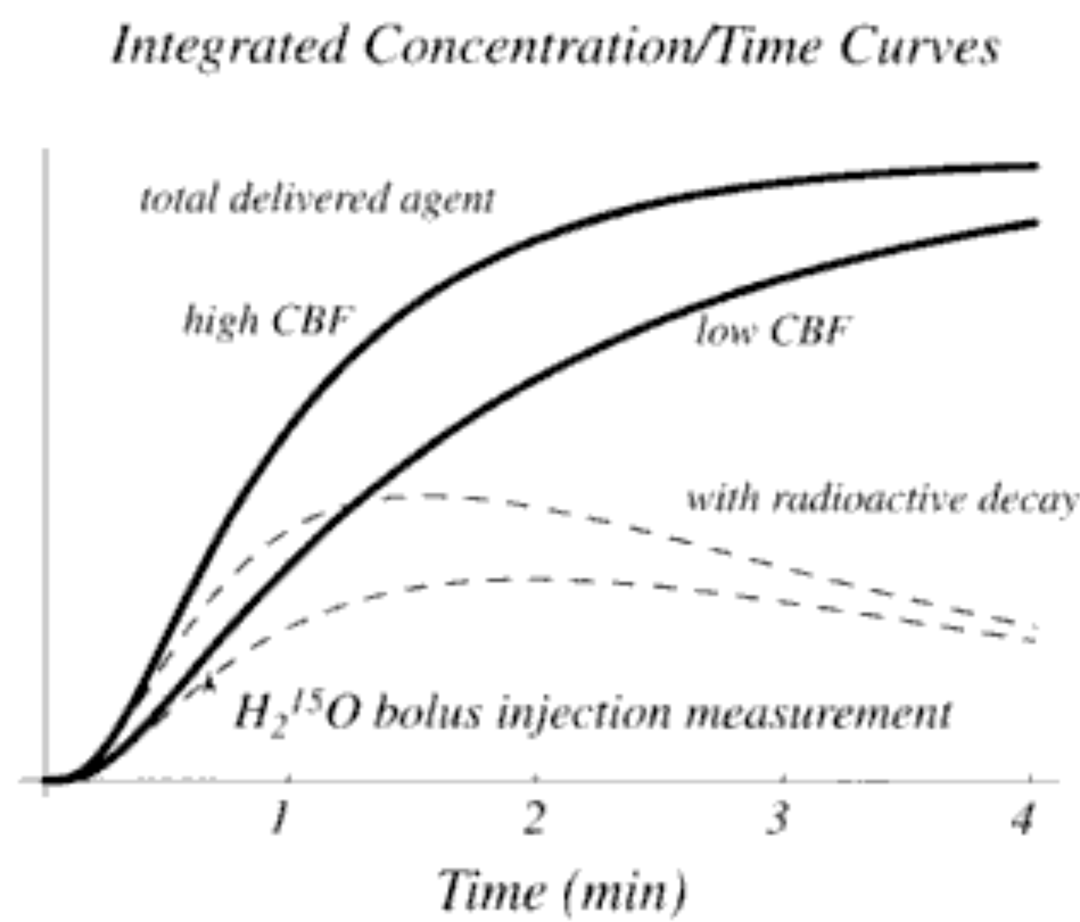

Population Assessment of Cognitive Subtraction

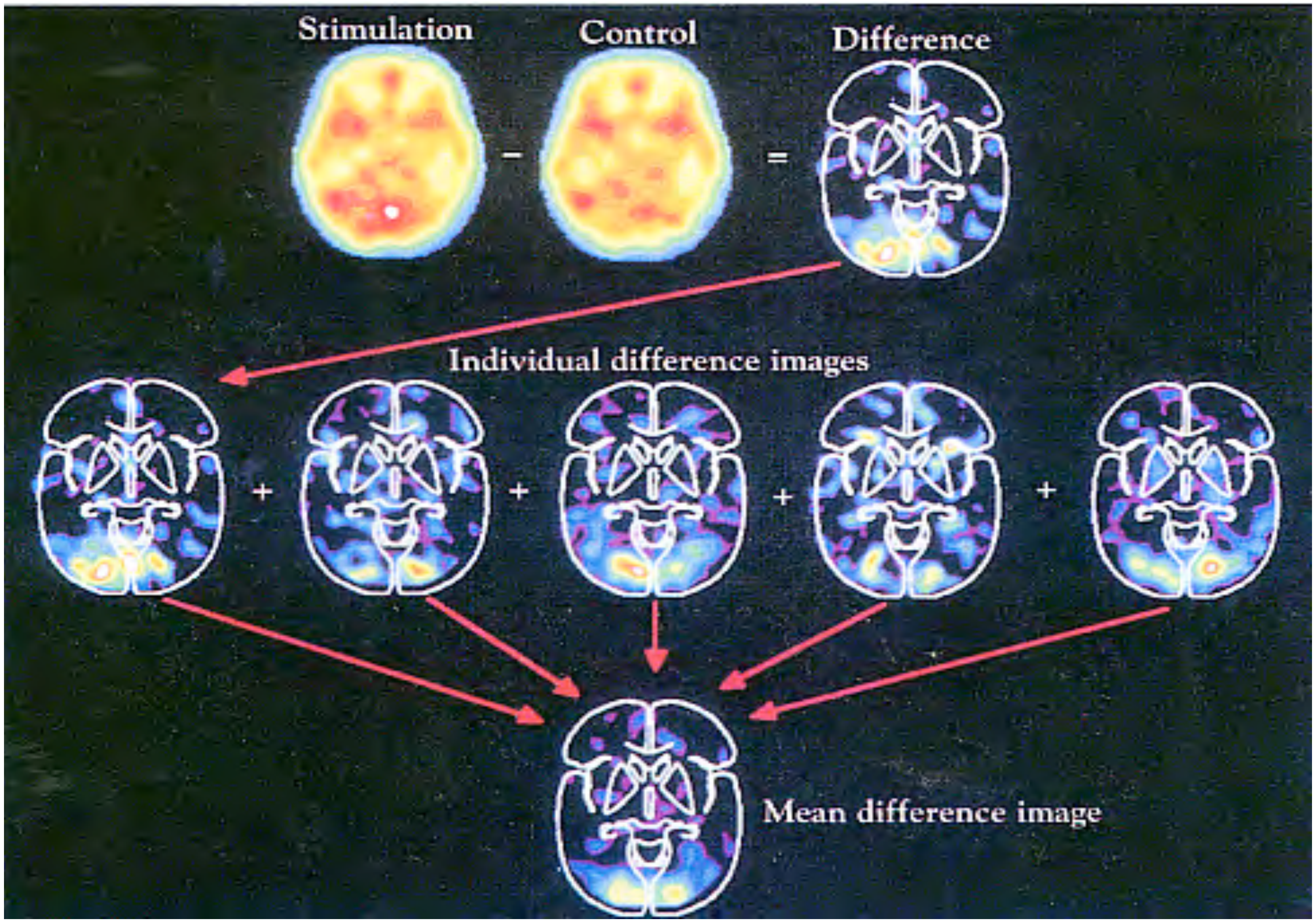

50-60% signal change

Mechanism of BOLD Functional MRI

Brain activity ↑

Oxygen consumption ↑

Cerebral blood flow ↑↑

Oxyhemoglobin ↑
Deoxyhemoglobin ↓

Magnetic susceptibility ↓

T2* ↑

MRI signal intesity ↑

3% signal change

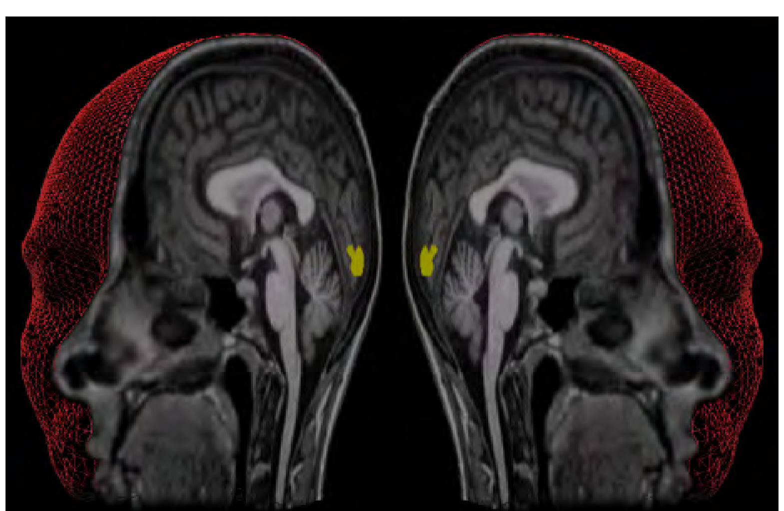

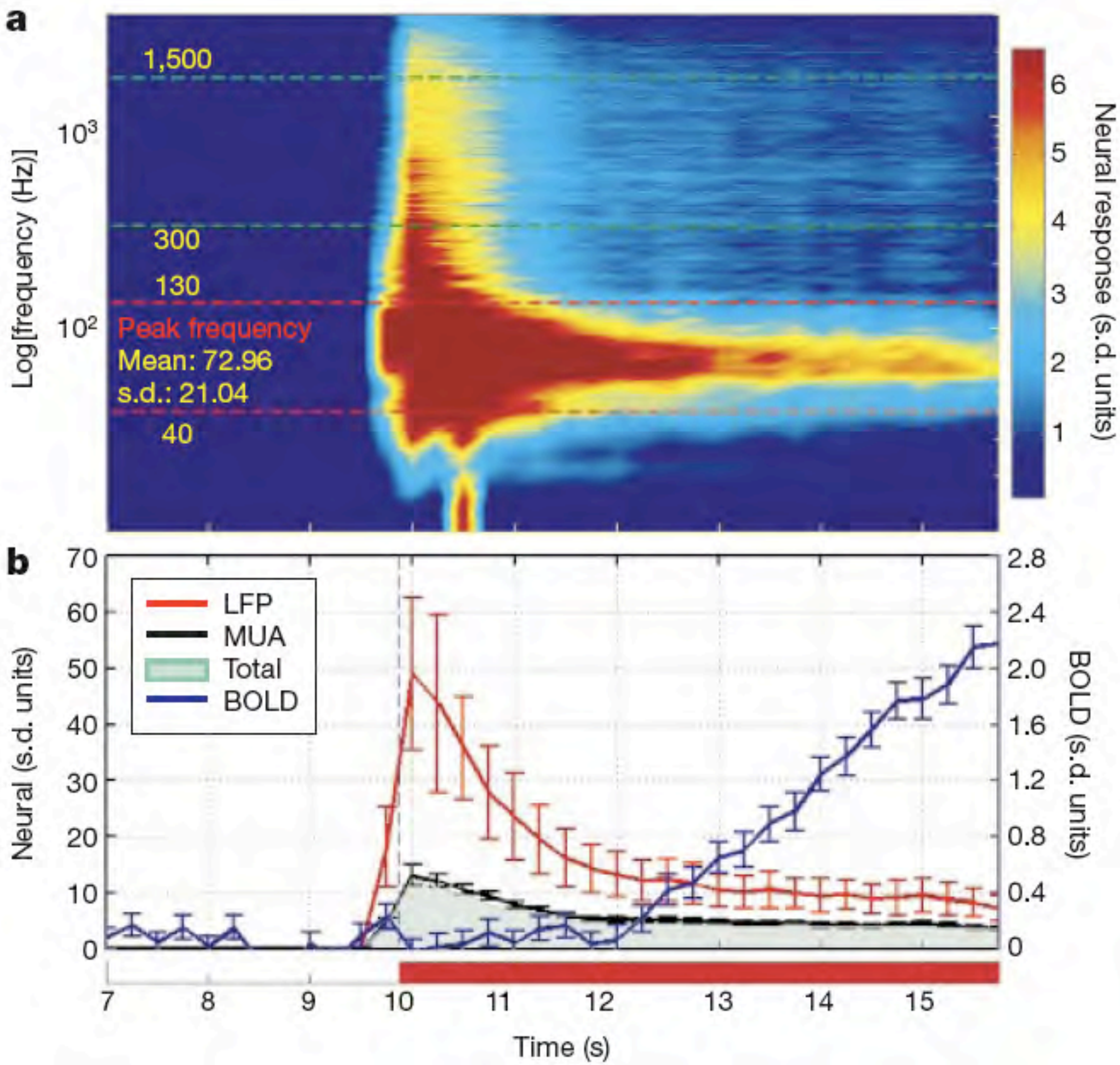
a
1,500
10^3
300
130
10^2
Peak frequency
Mean: 72.96
s.d.: 21.04
40
Log[frequency (Hz)]
Neural response (s.d. units)
b
LFP
MUA
Total
BOLD
Neural (s.d. units)
BOLD (s.d. units)
Time (s)

J. Neurosci., July 1, 1996, 16(13):4207–4221

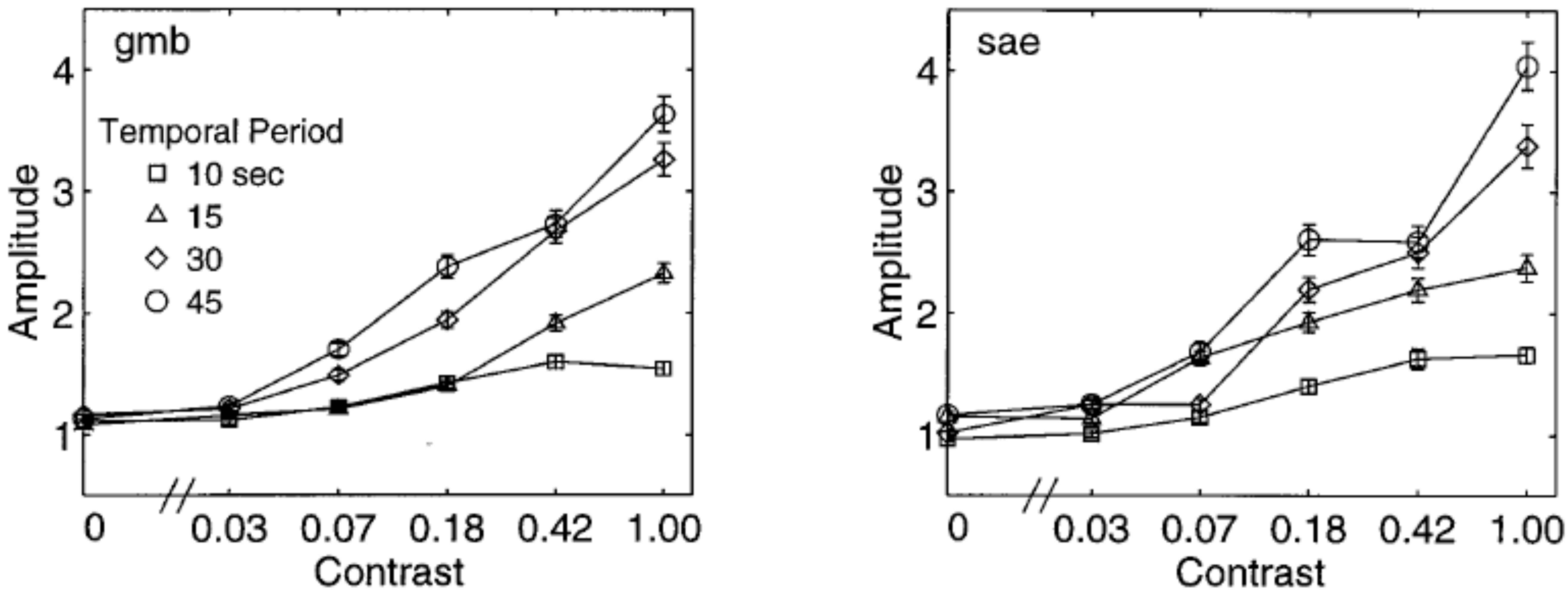

Comparison of hemodynamic response nonlinearity across primary cortical areas

David A. Soltysik,[a,*] Kyung K. Peck,[b,1] Keith D. White,[c]
Bruce Crosson,[d] and Richard W. Briggs[b,2]

NeuroImage 22 (2004) 1117–1127

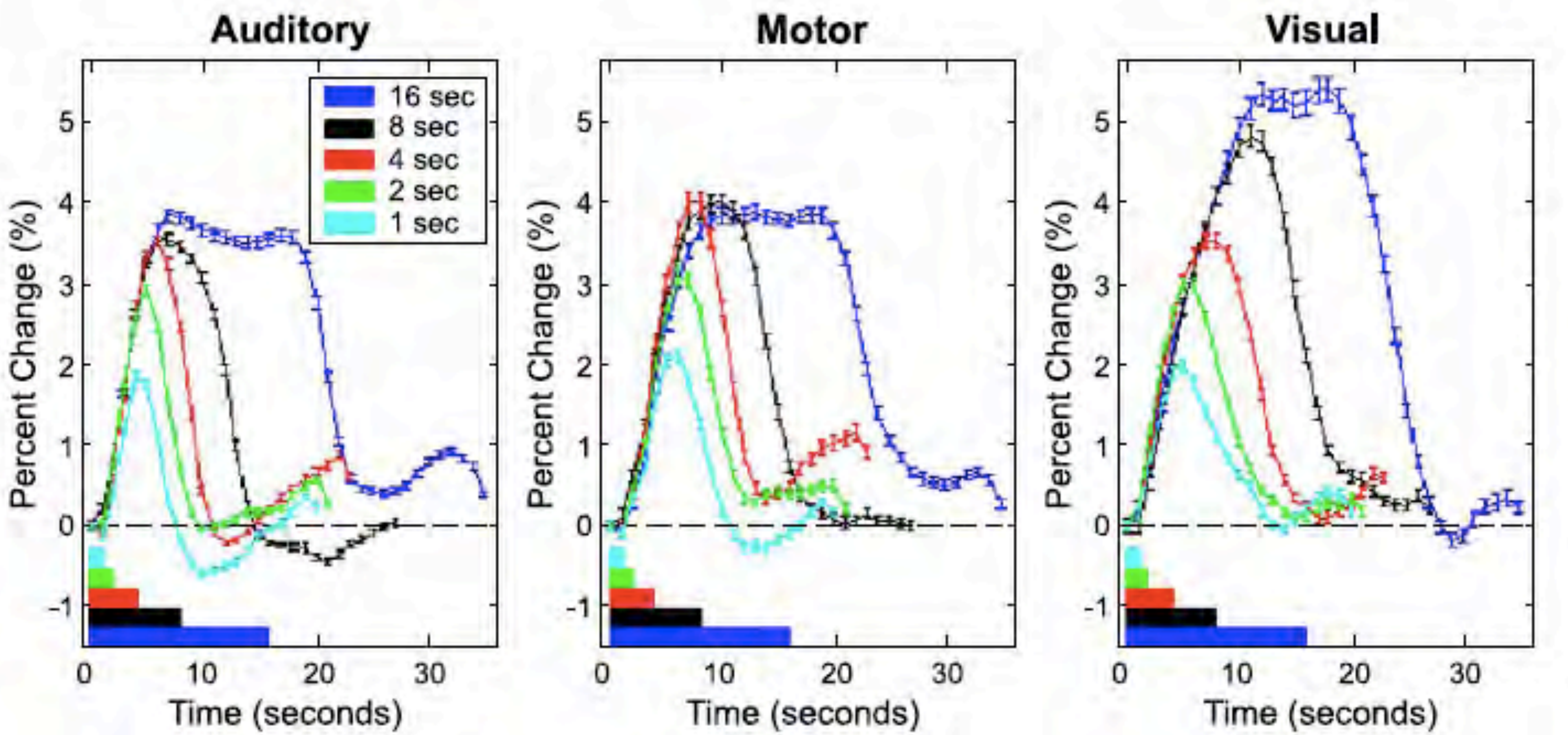

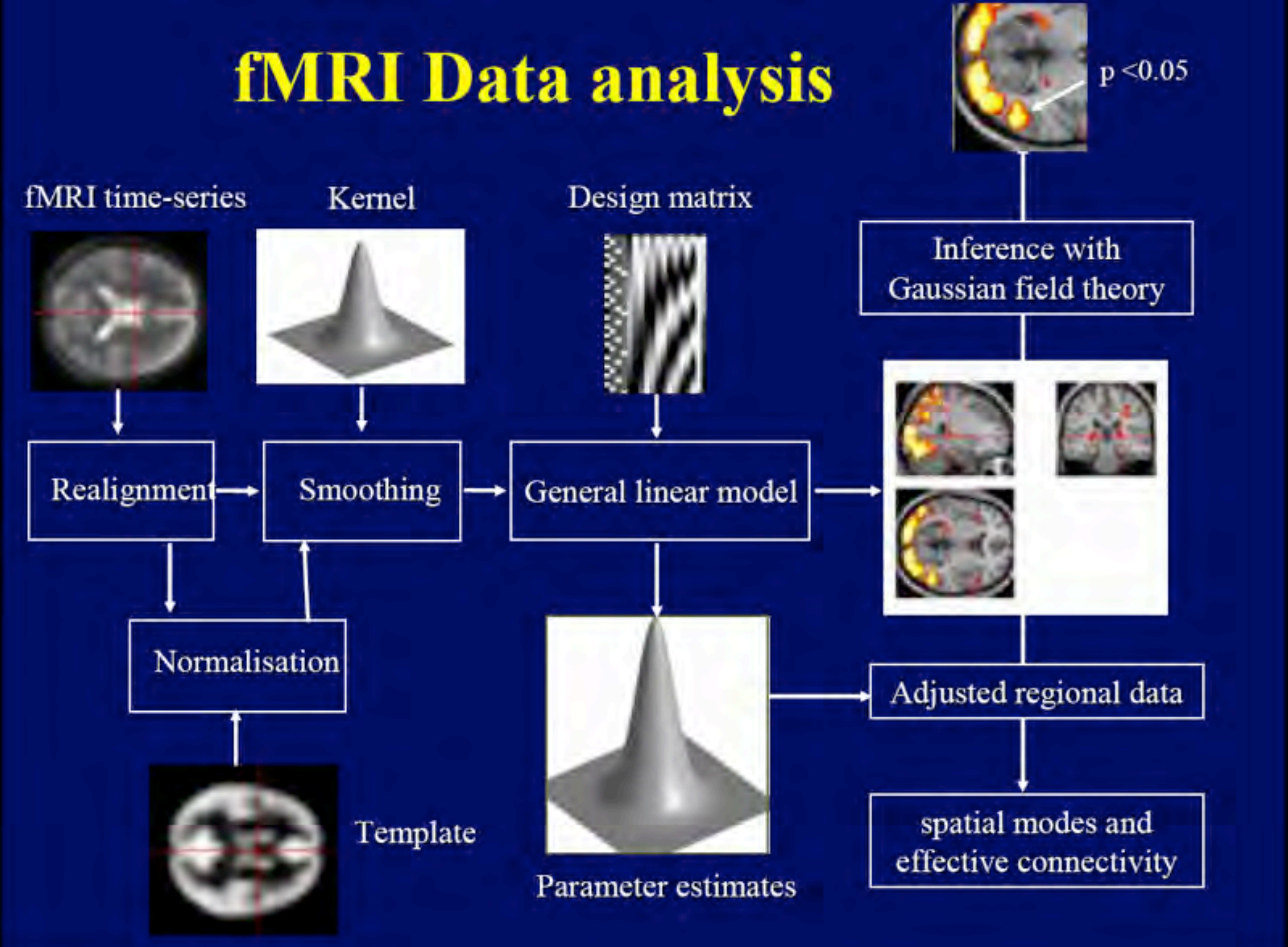
fMRI Data analysis
p <0.05
fMRI time-series
Kernel
Design matrix
Inference with Gaussian field theory
Realignment
Smoothing
General linear model
Normalisation
Adjusted regional data
Template
Parameter estimates
spatial modes and effective connectivity

Low Frequency Noise: F-test of basis functions

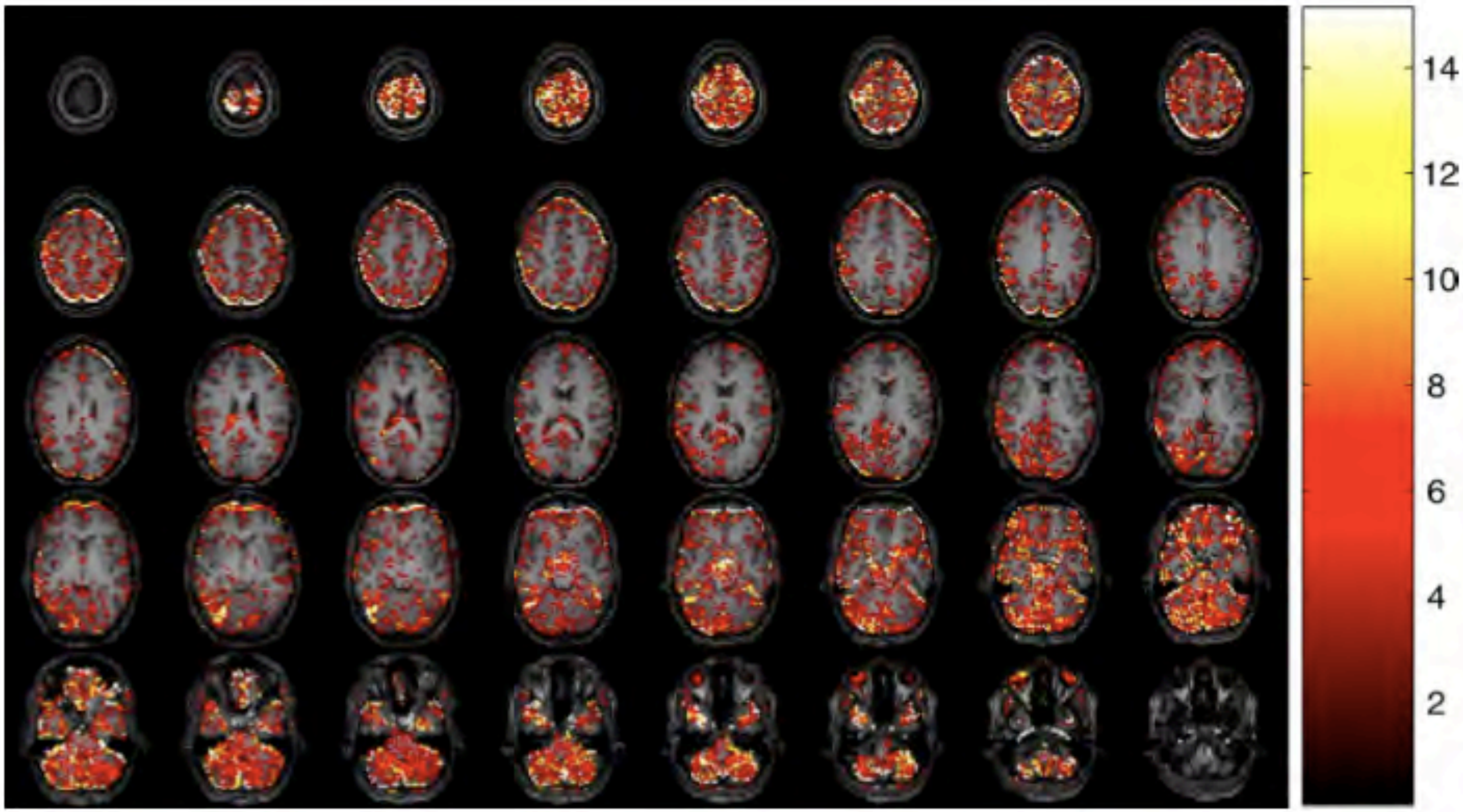

Residual Movement Effects

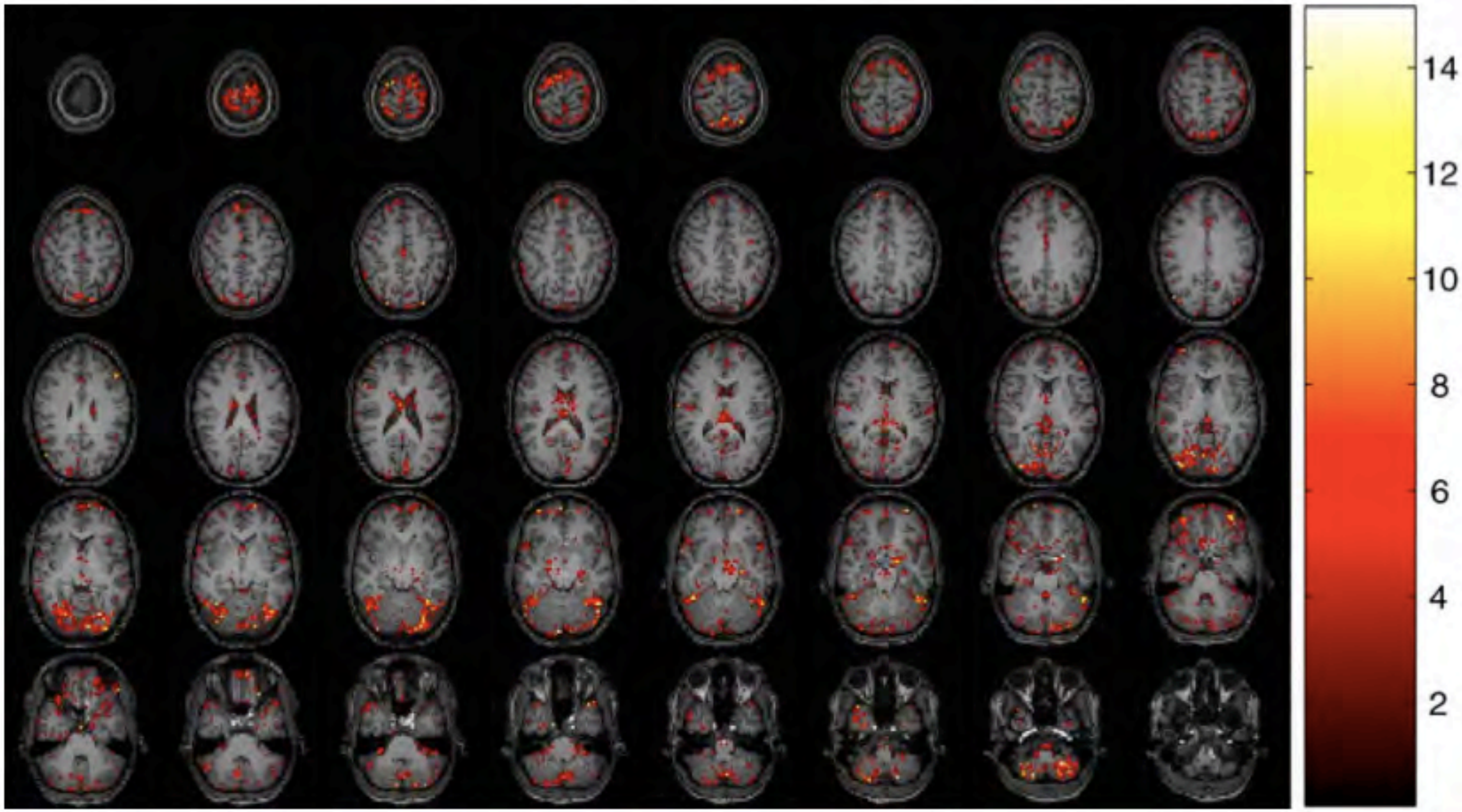

Respiration Induced Noise

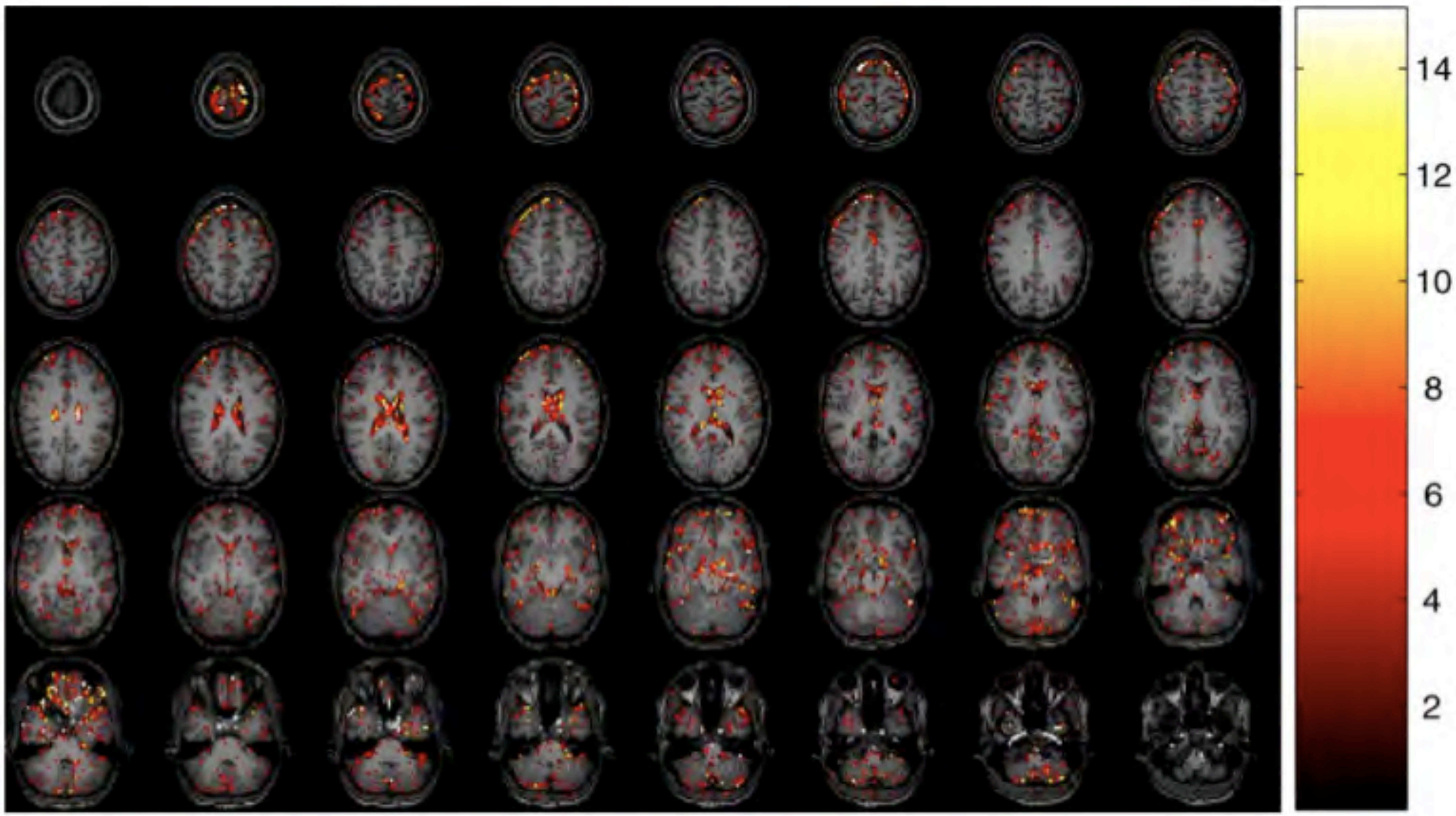

Cardiac Induced Noise

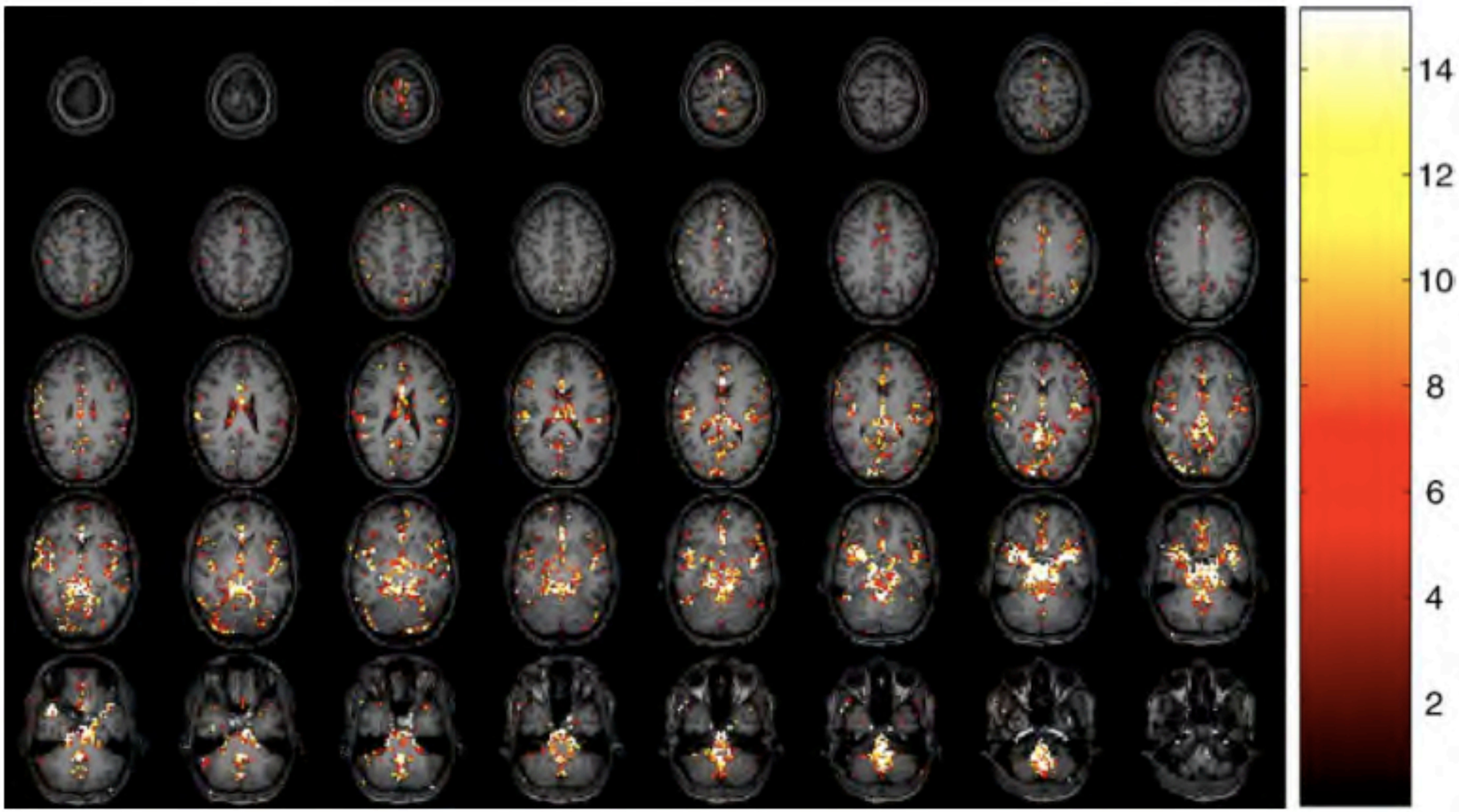

Visual Activation

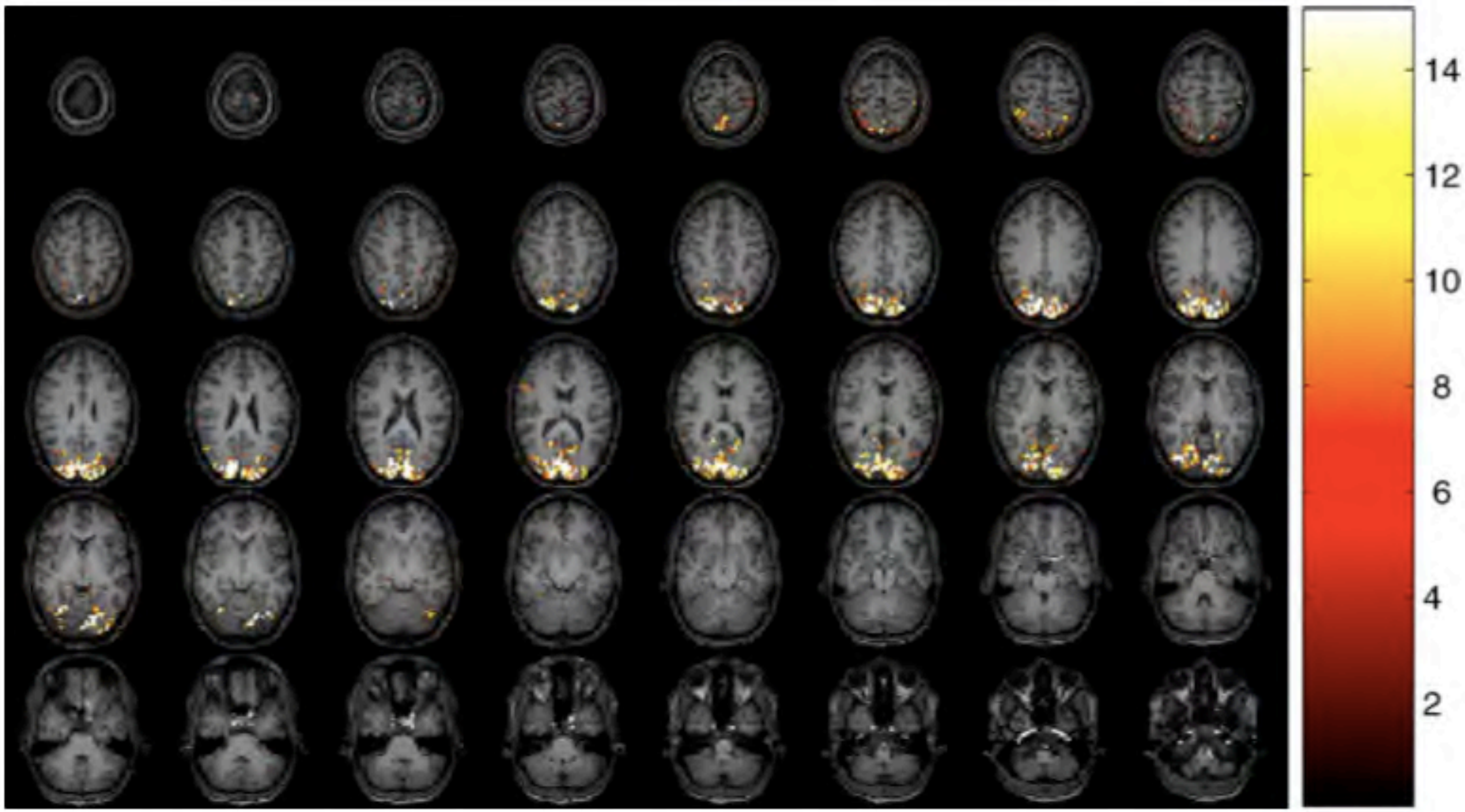

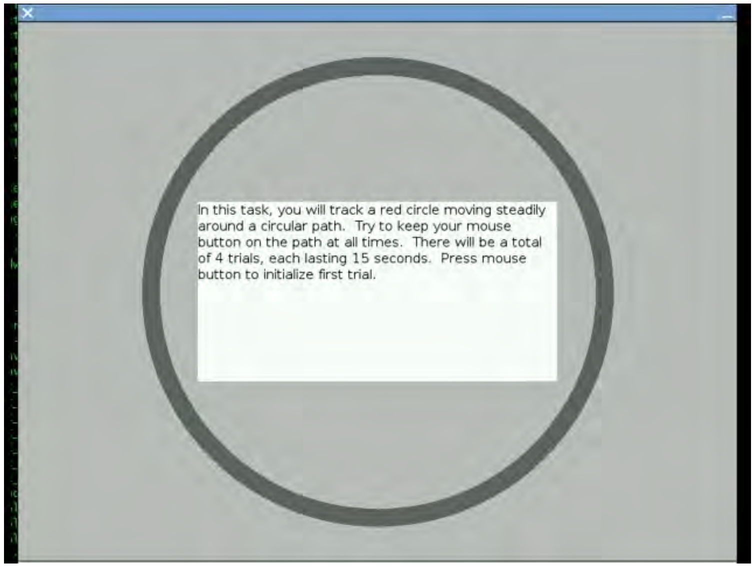

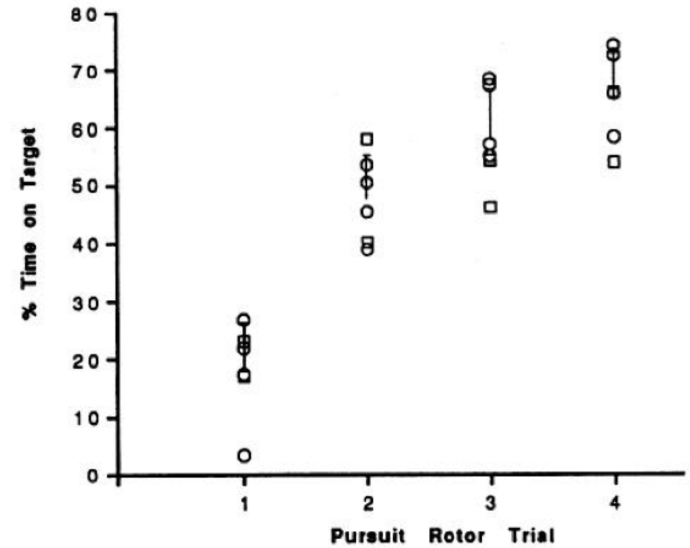

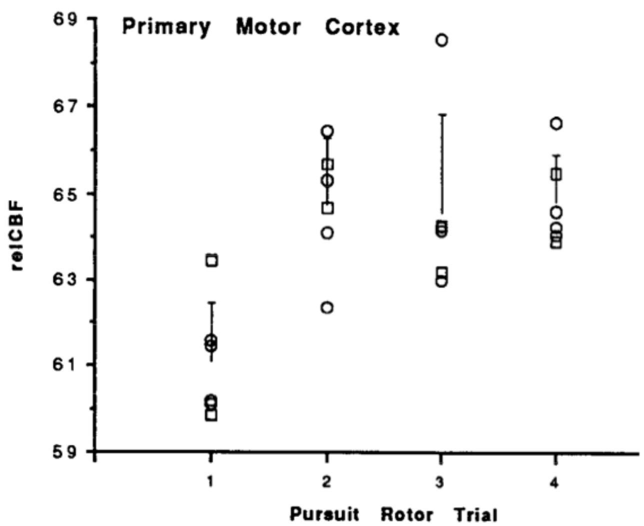

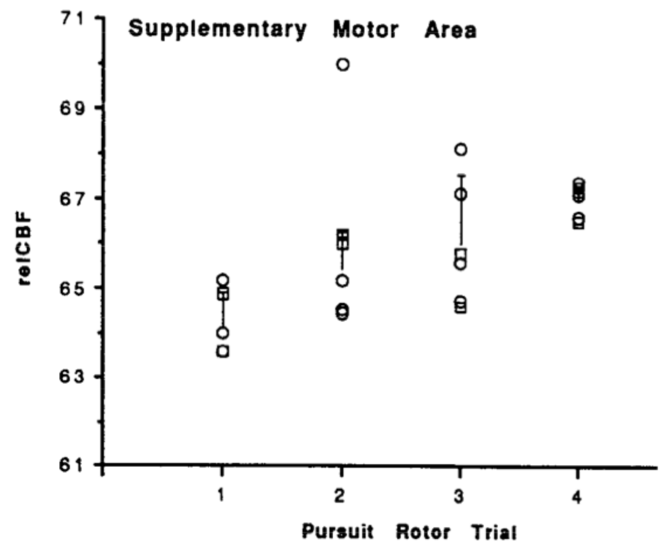

The Journal of Neuroscience, July 1992, *12*(7): 2542–2548

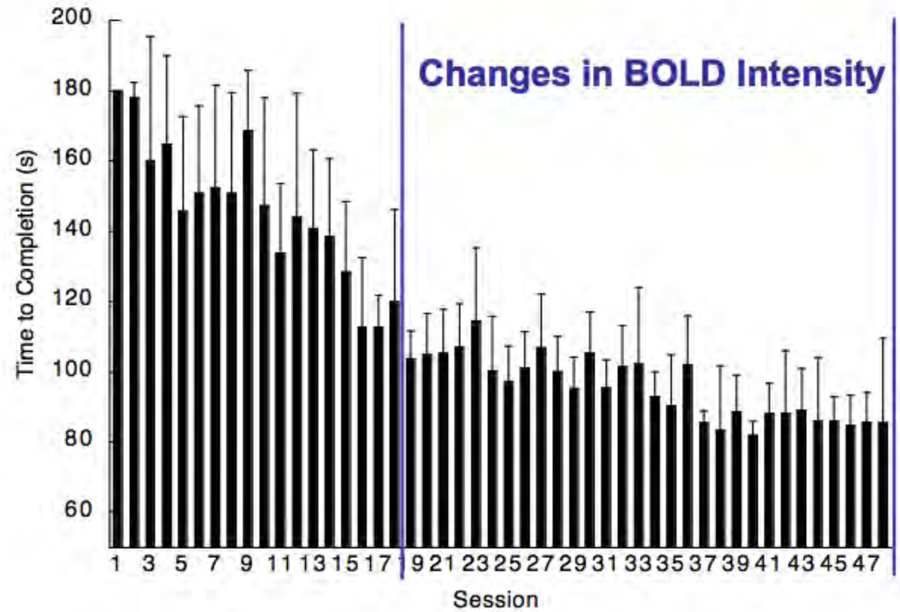

Changes in BOLD Intensity
Time to Completion (s)
200
180
160
140
120
100
80
60
1 3 5 7 9 11 13 15 17 19 21 23 25 27 29 31 33 35 37 39 41 43 45 47
Session

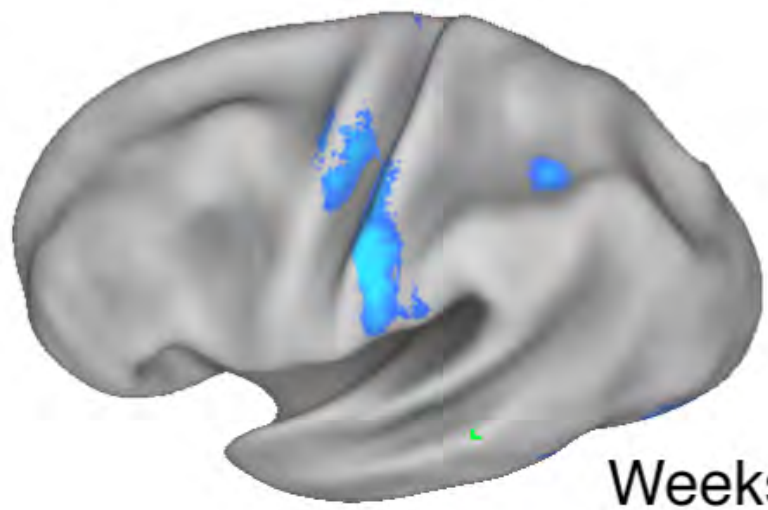

Weeks 19-48

There is no procedural memory SYSTEM

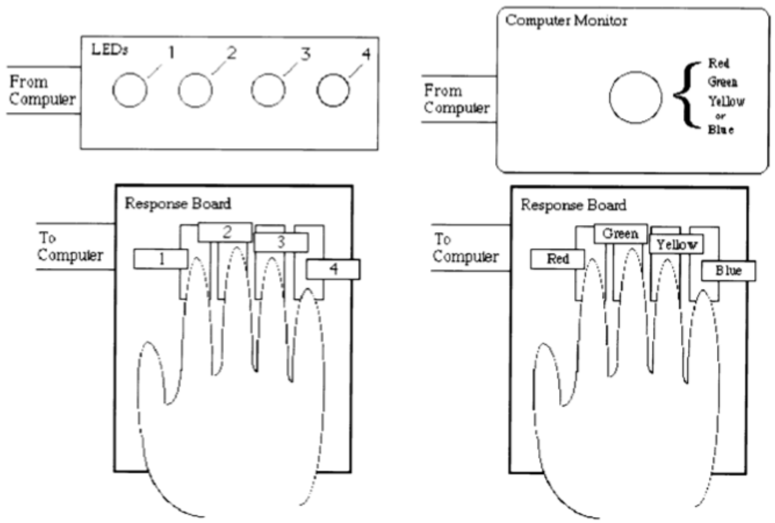

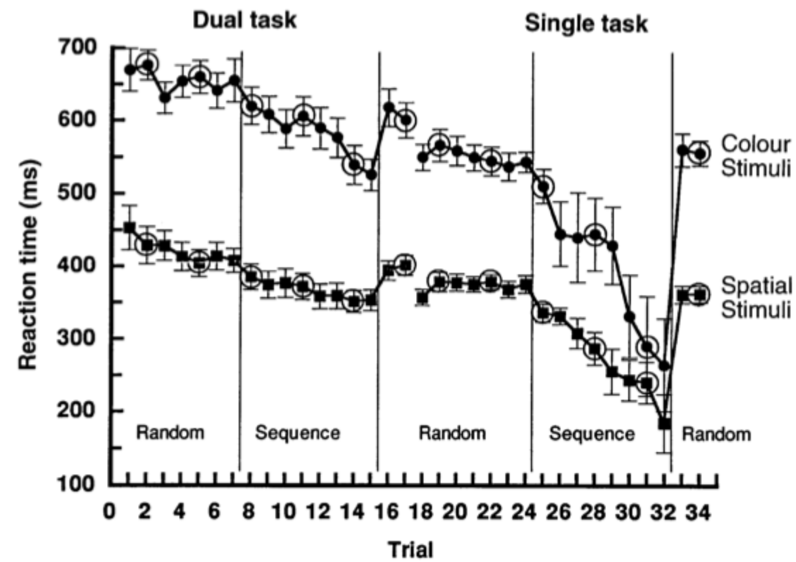

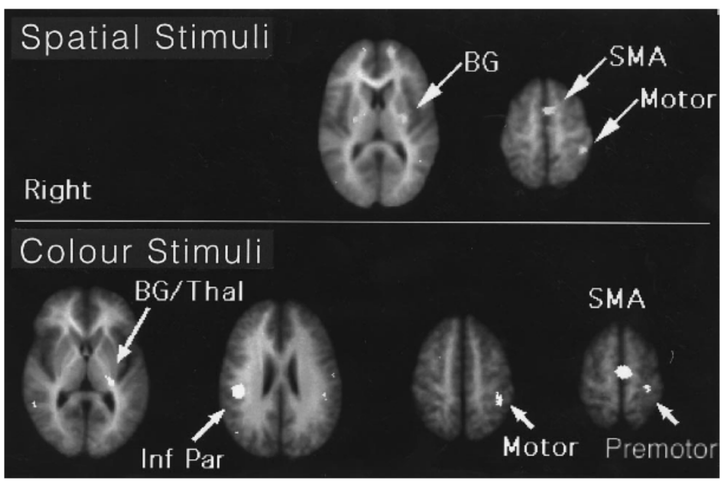

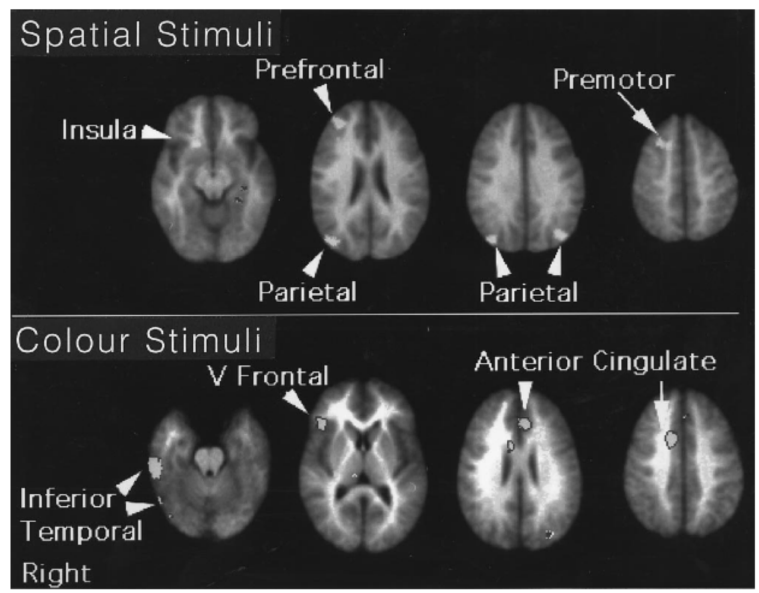

Brain (1997), **120**, 123–140

Large-Scale Organization of Connectivity

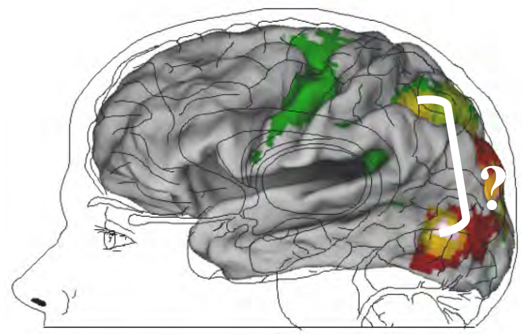

Structure

Function

White Matter
Tracts Form
'Hard-wired
Connectivity'

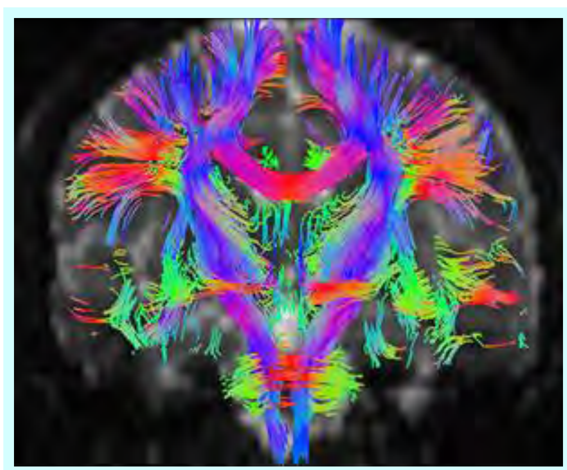

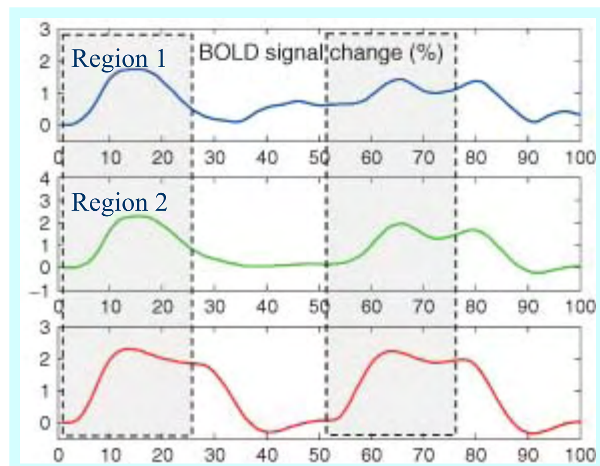

Functional
Association
Between Time
Series Forms
'Functional
Connectivity'

The Predictive Value of Changes in Effective Connectivity for Human Learning

C. Büchel,* J. T. Coull, K. J. Friston

Visual associative learning: Object identification and location

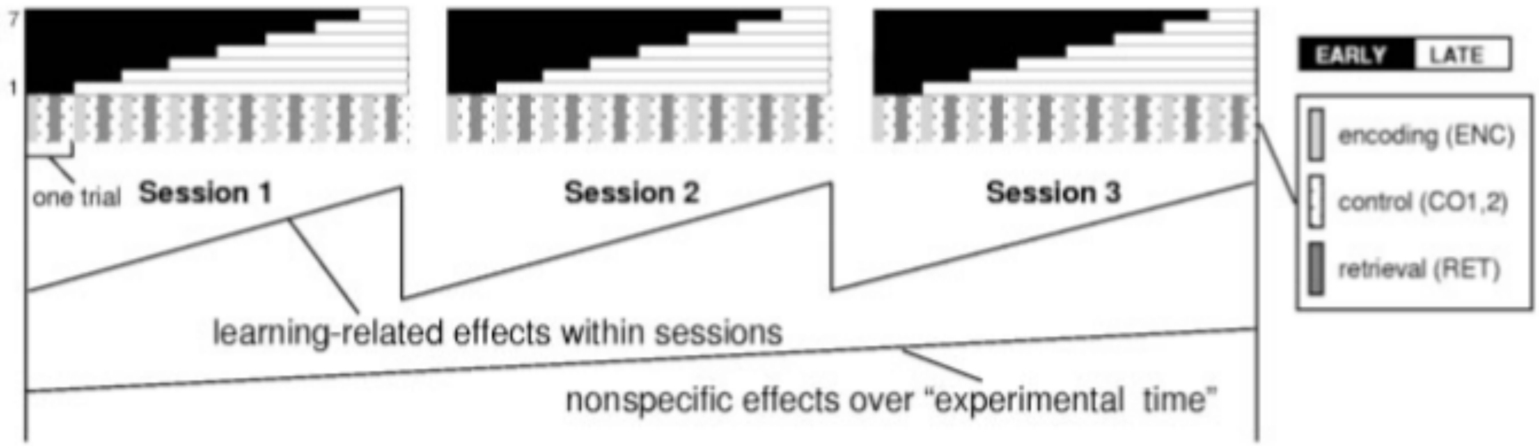

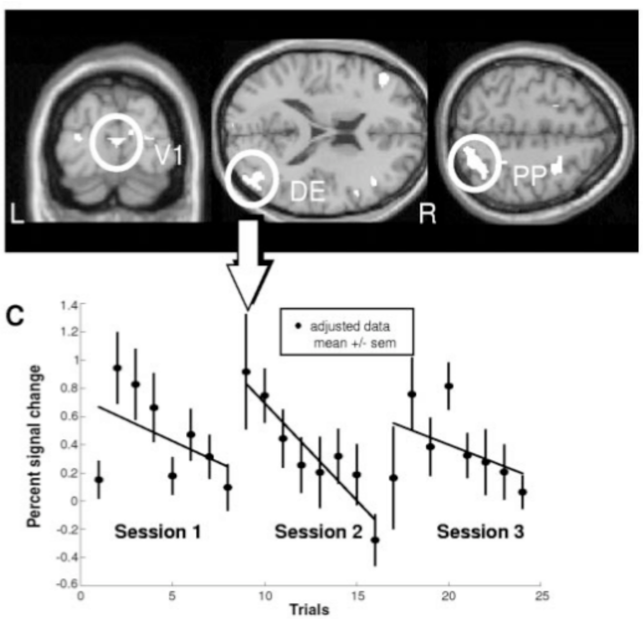

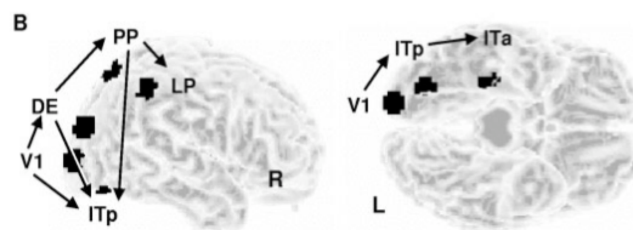

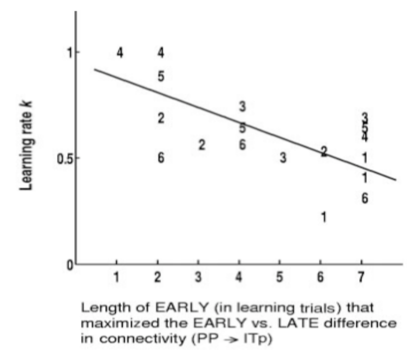

Modularity in Function

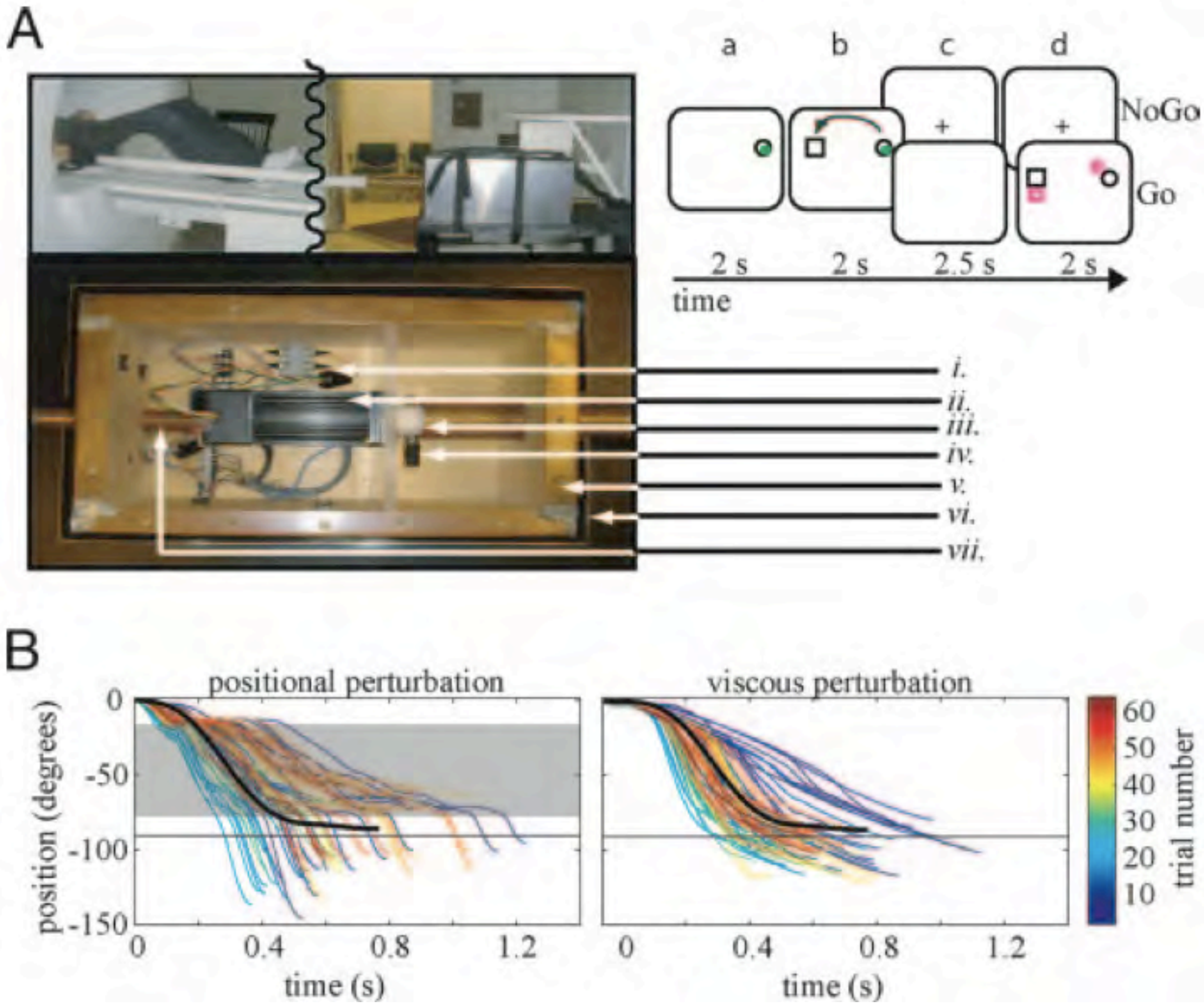

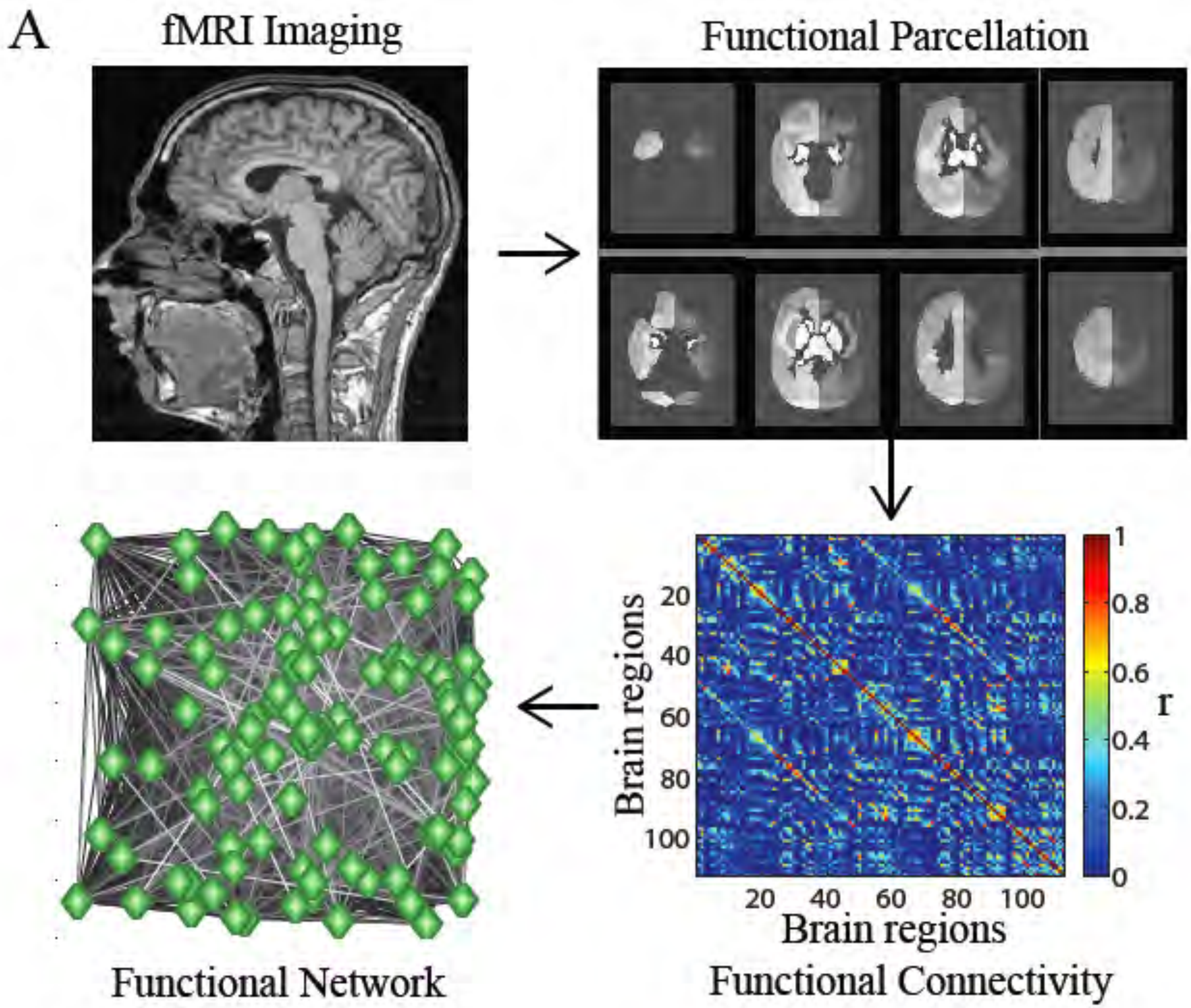
A
fMRI Imaging
Functional Parcellation
Functional Connectivity
Brain regions
20
40
60
80
100
Brain regions
20
40
60
80
100
r
0
0.2
0.4
0.6
0.8
1
Functional Network

Modularity in Function

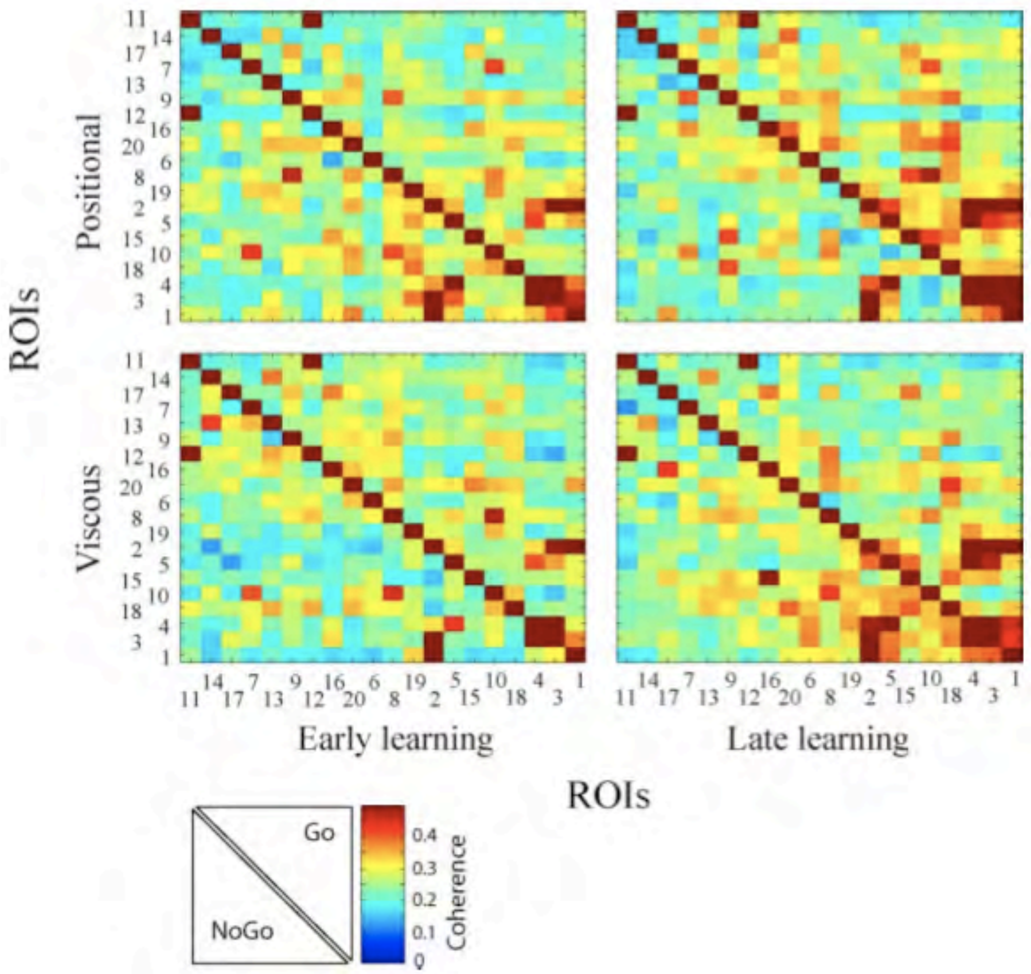

Step 1

Step 2

Step 3

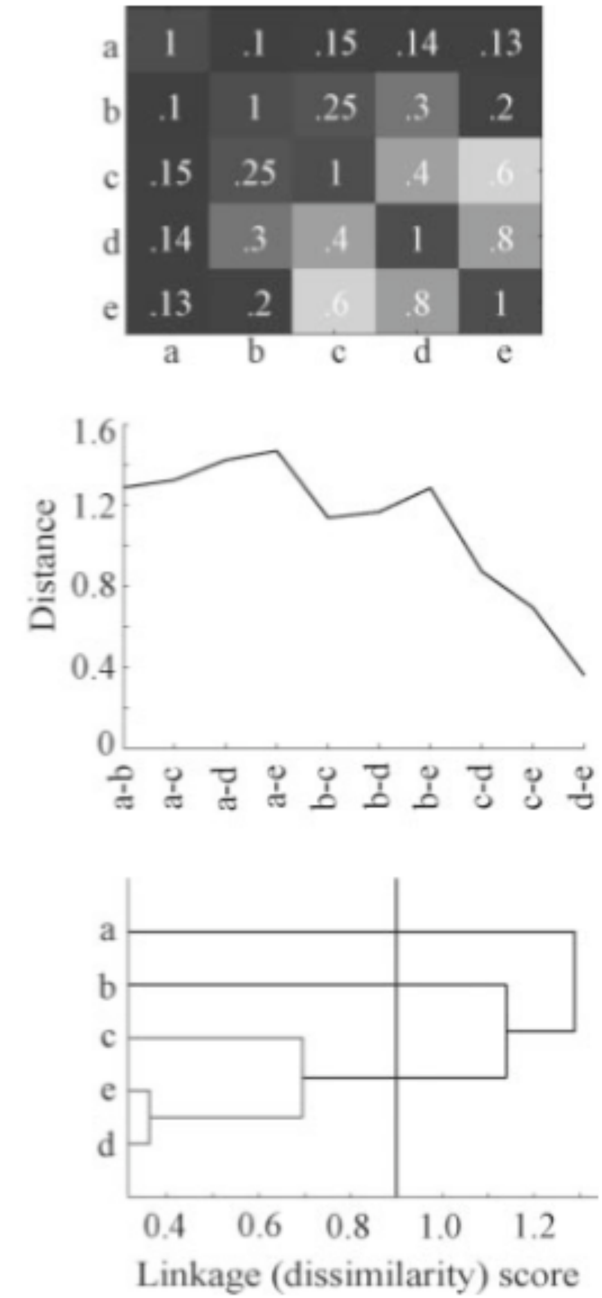

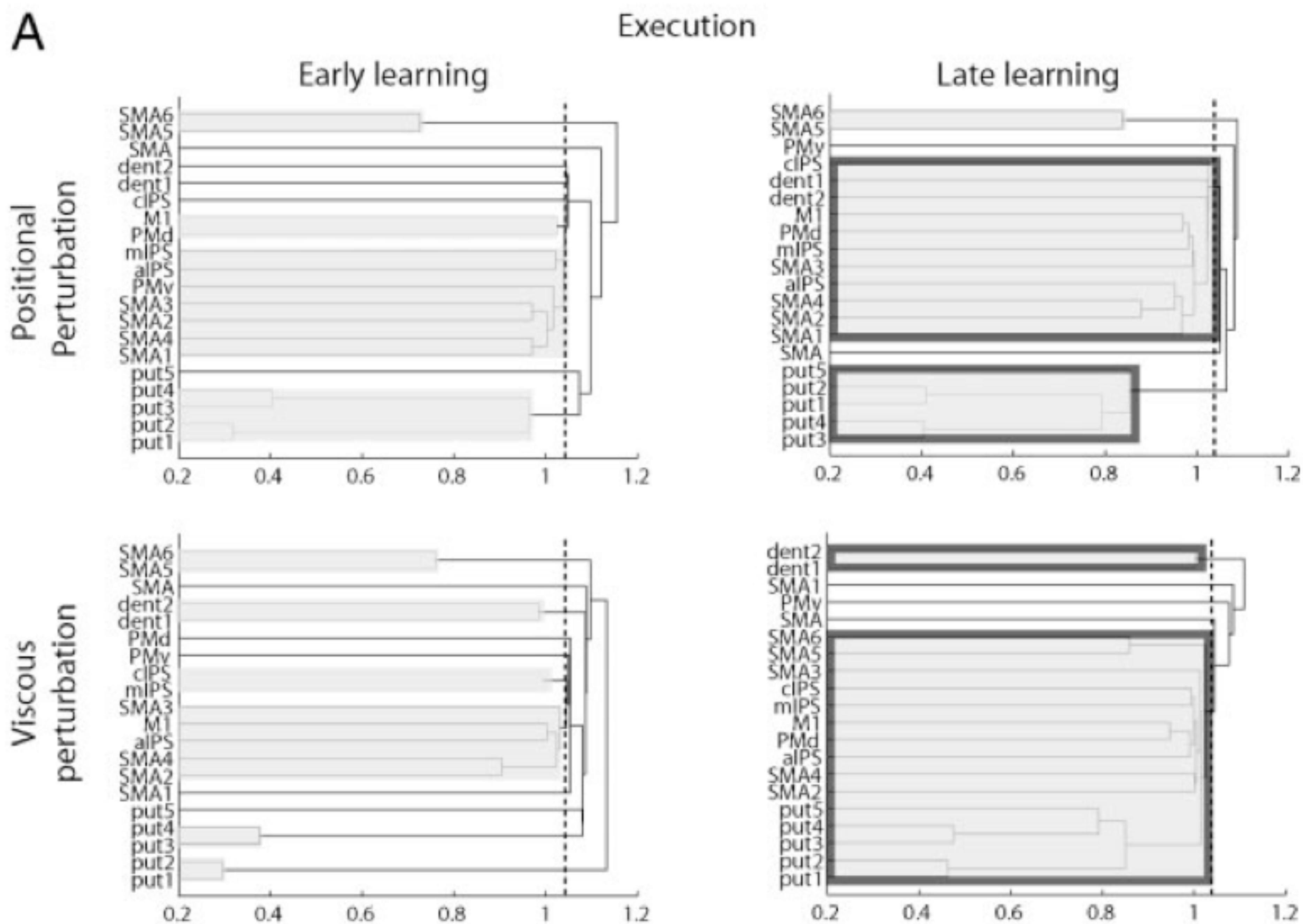
A
Execution
Early learning
Late learning
Positional Perturbation
Viscous perturbation
SMA6
SMA5
SMA
dent2
dent1
cIPS
M1
PMd
mIPS
aIPS
PMv
SMA3
SMA2
SMA4
SMA1
put5
put4
put3
put2
put1
0.2
0.4
0.6
0.8
1
1.2

Building Cortical Connectivity Maps

from task based fMRI

How do we build a brain network?

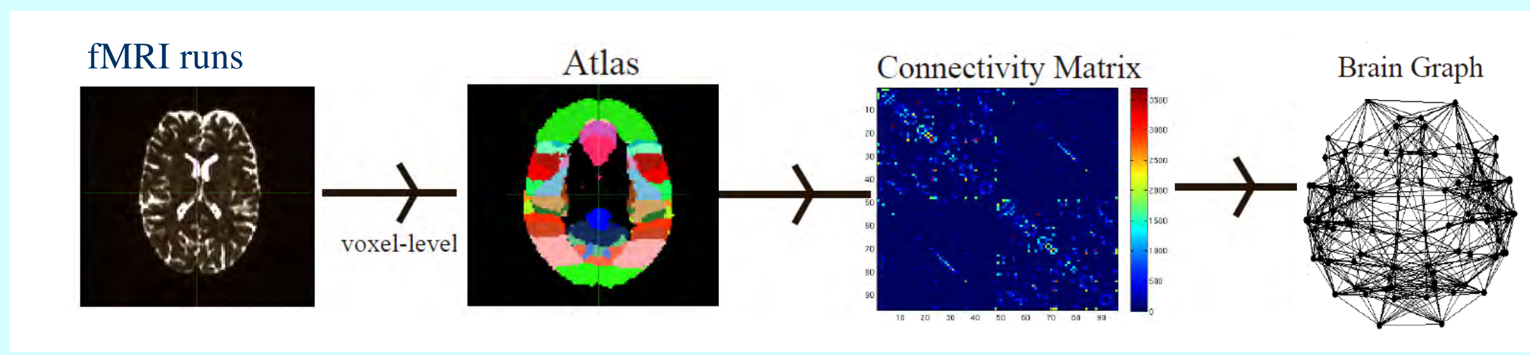

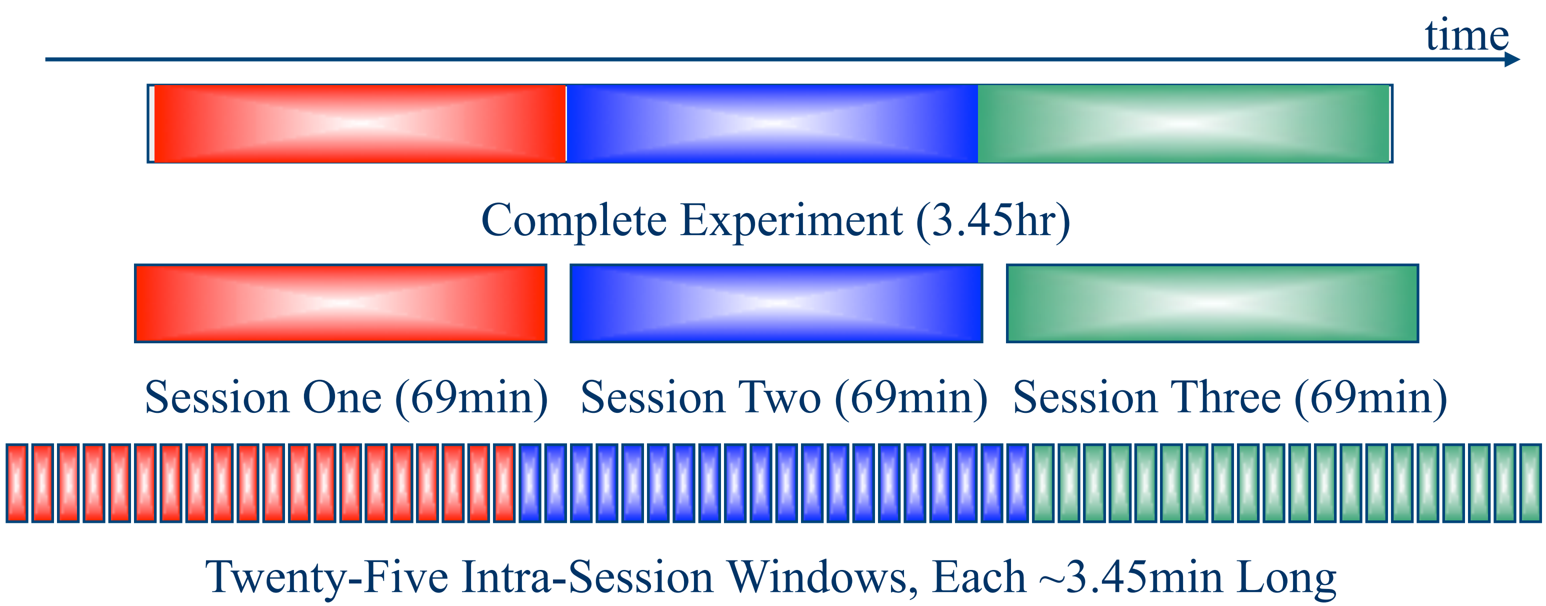

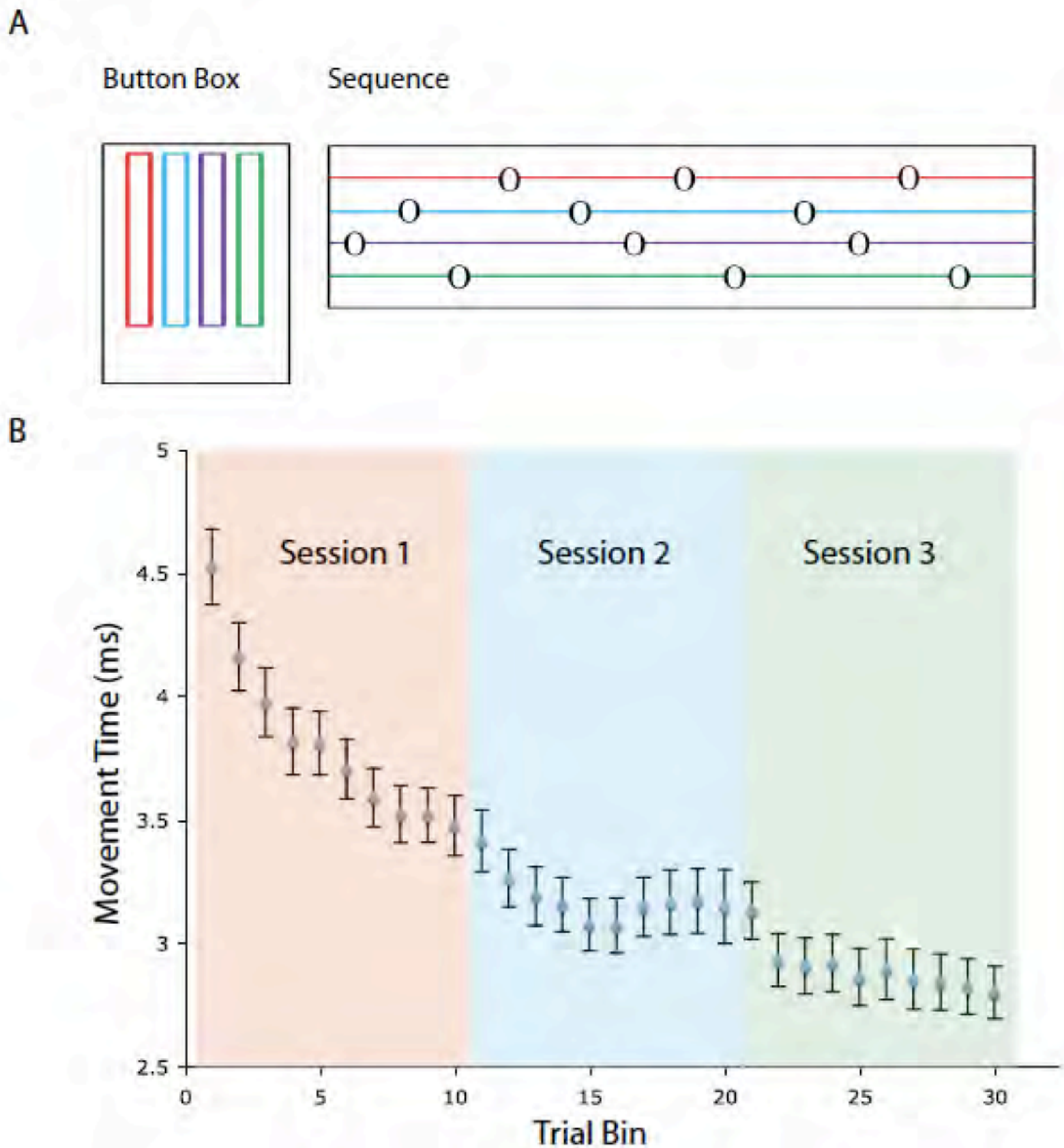
A
Button Box
Sequence
B
Session 1
Session 2
Session 3
Movement Time (ms)
Trial Bin
5
4.5
4
3.5
3
2.5
0
5
10
15
20
25
30

Modularity in the Complete Experiment

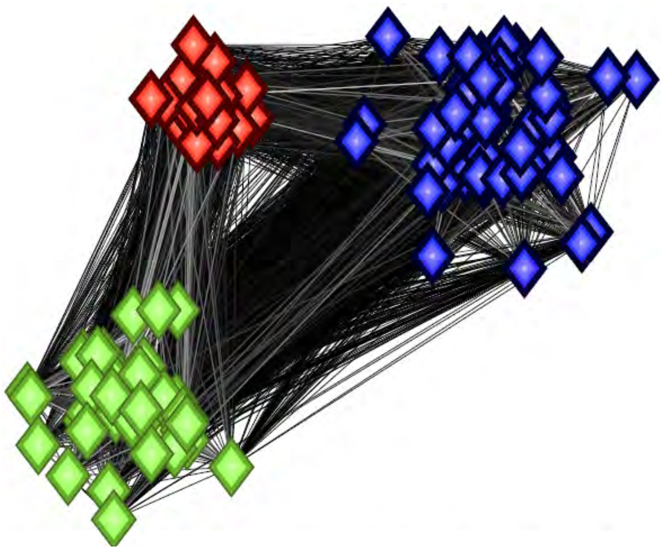

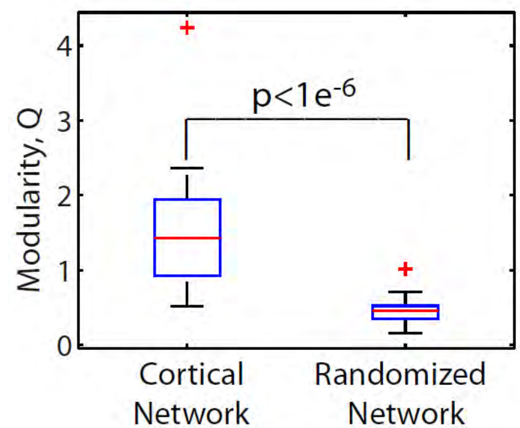

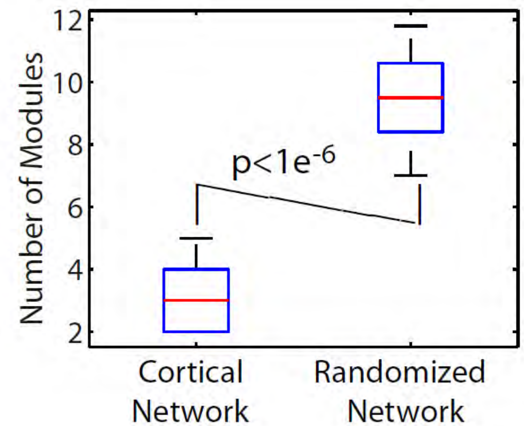

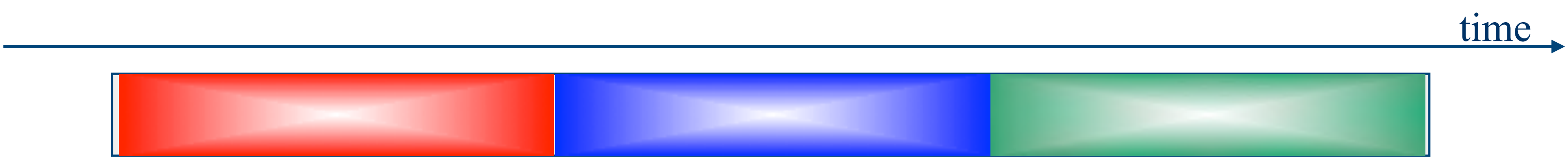

Complete Experiment (3.45hr)

Modularity in Individual Sessions

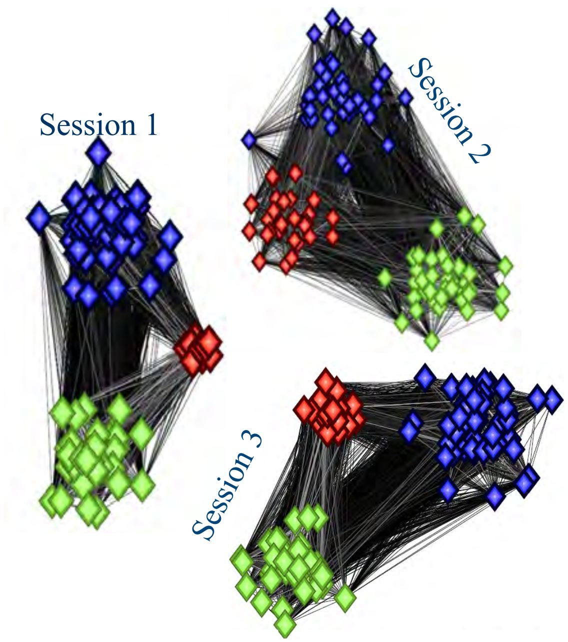

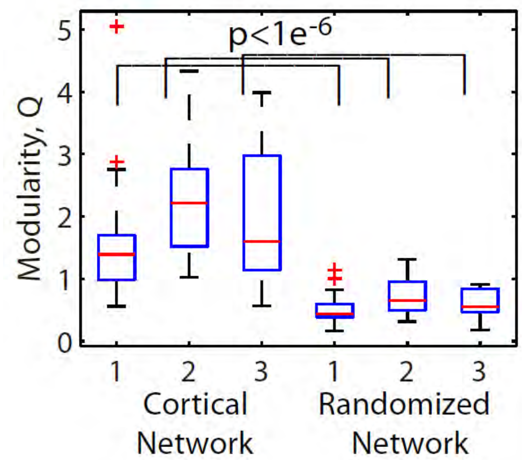

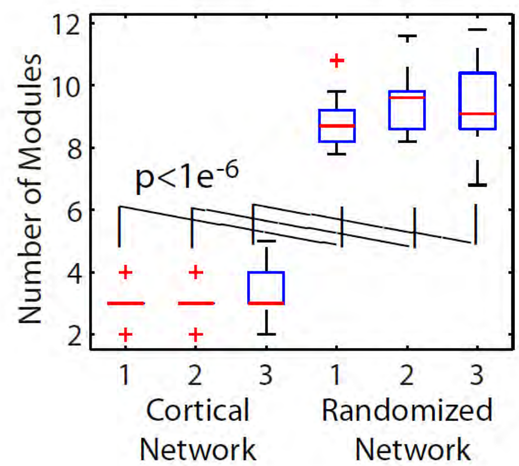

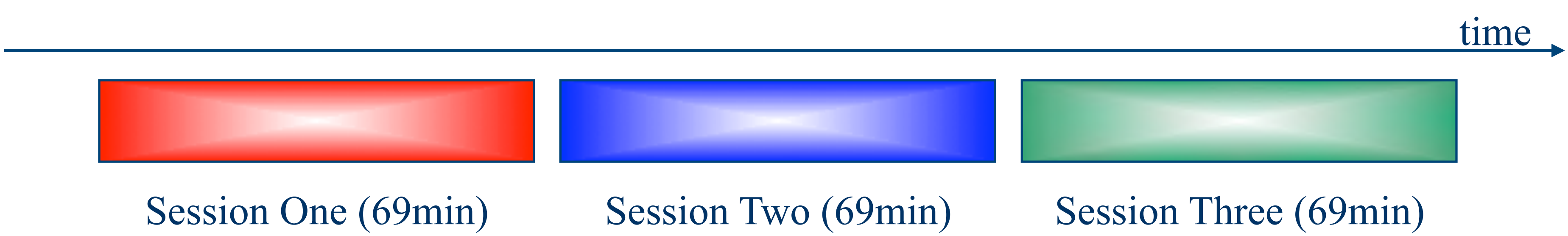

Modularity in Individual Time Windows

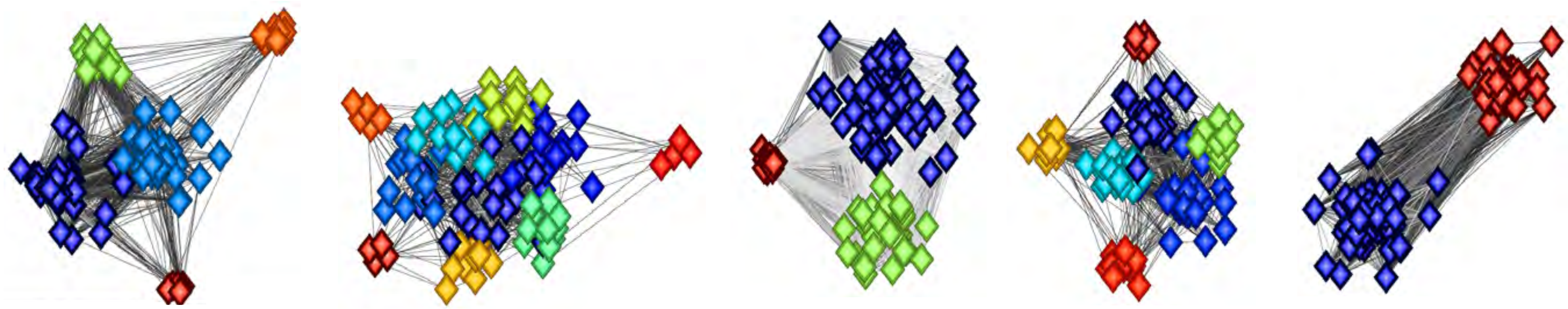

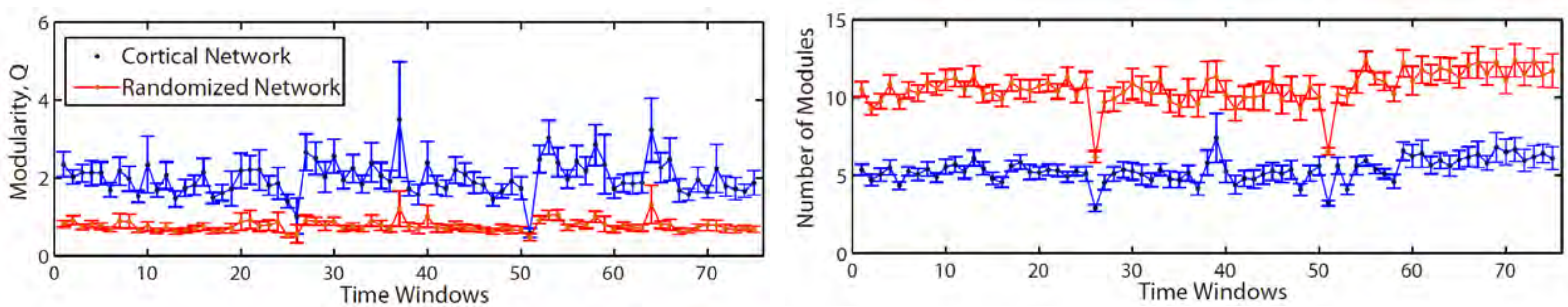

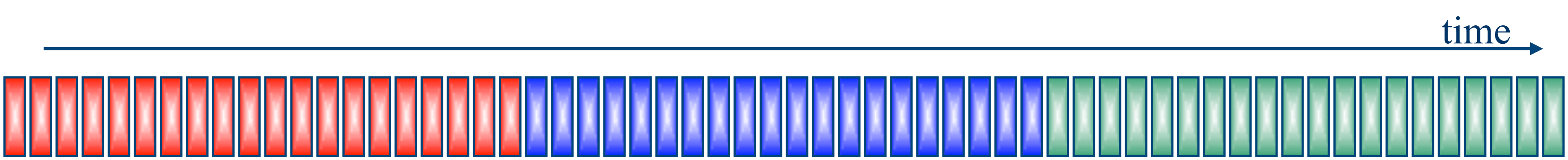

Twenty-Five Intra-Session Windows, Each ~3.45min Long

Temporal Evolution of Modular Architecture

What if we want to not only measure the temporal *dependence* of modular architecture, but also the temporal *evolution* of that architecture? We need a new framework.

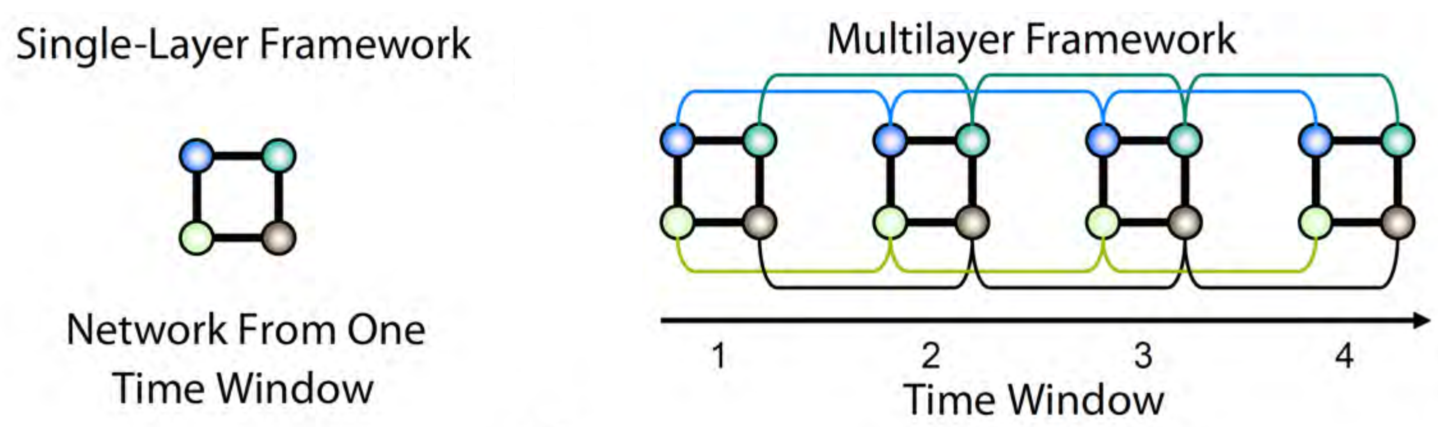

Community detection can now be performed on this linked multilayered network to find modules with longevity in the temporal domain.

Community Structure in Time-Dependent, Multiscale, and Multiplex Networks

Peter J. Mucha,[1,2]* Thomas Richardson,[1,3] Kevin Macon,[1] Mason A. Porter,[4,5] Jukka-Pekka Onnela[6,7]

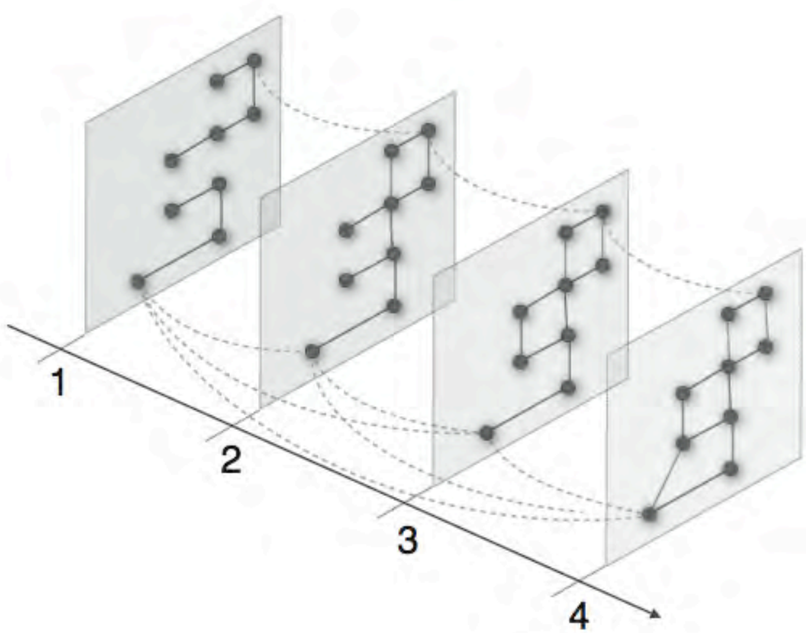

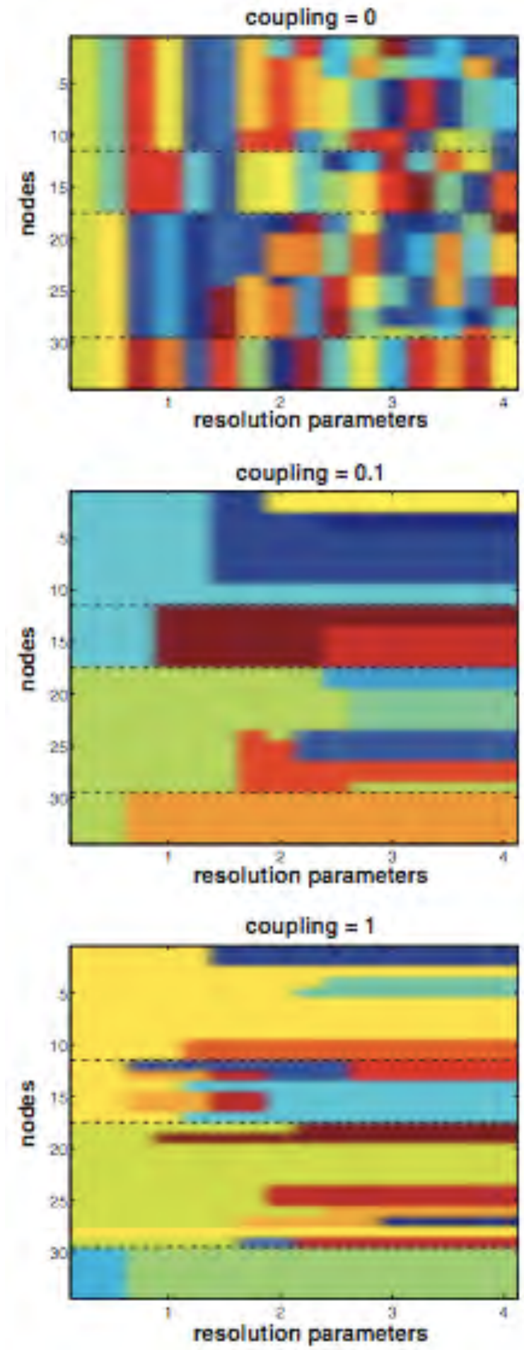

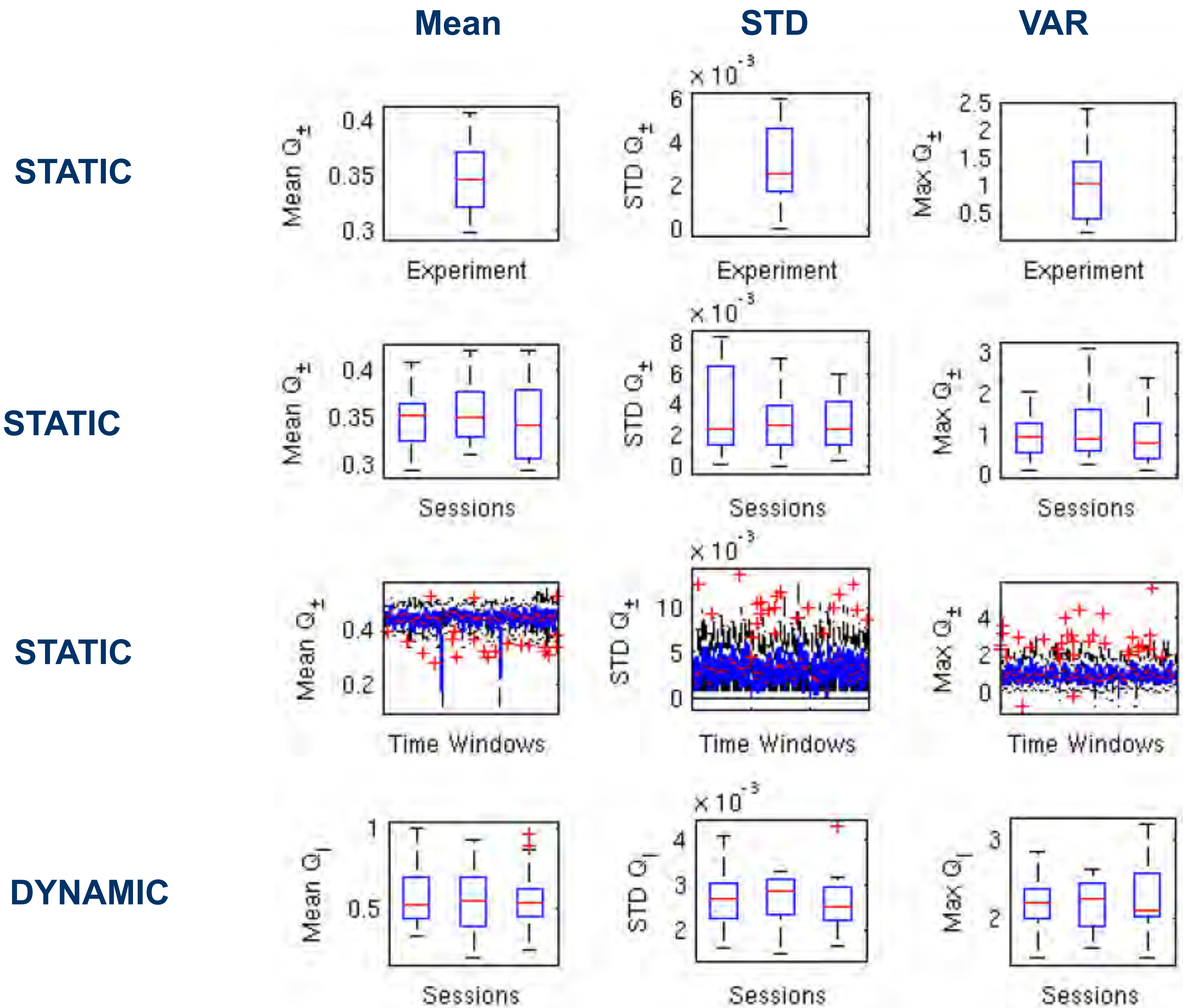
Mean
STD
VAR
STATIC
STATIC
STATIC
DYNAMIC
Mean Q±
STD Q±
Max Q±
Mean Q|
STD Q|
Max Q|
× 10^-3
Experiment
Sessions
Time Windows

Temporal Evolution of Modular Architecture

Statistical Testing

1) The topological organization of cortical connectivity is highly structured

2) Diverse brain regions perform distinct non-interchangeable tasks throughout the experiment

3) The evolution of modular architecture in human brain function is cohesive in time.

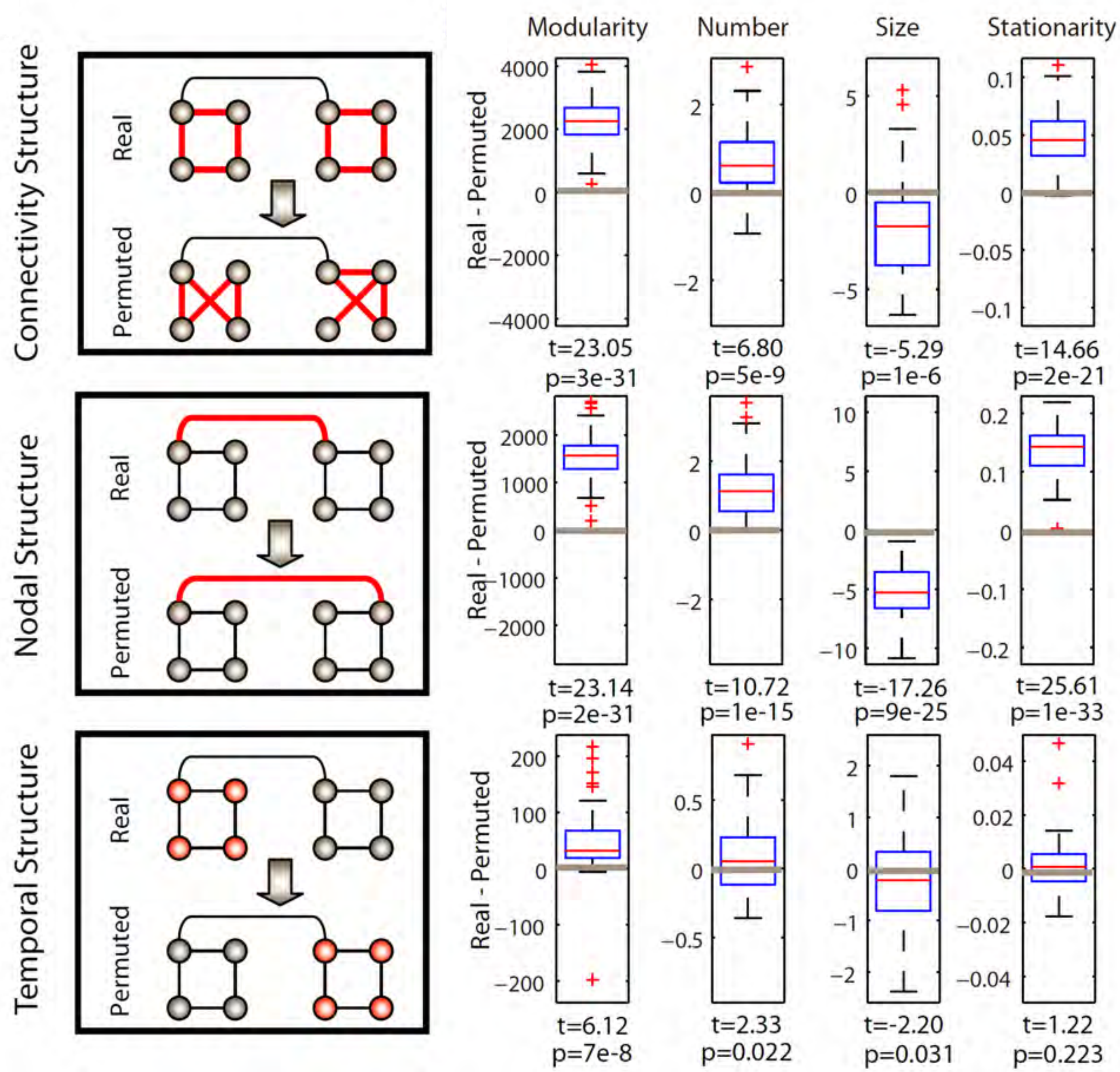

Flexibility of Module Composition

Now that we know there is significant structure here, we can ask how it relates to learning over the three scanning sessions.

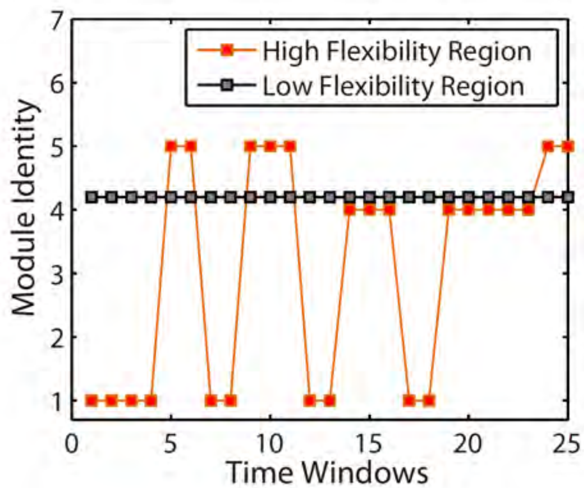

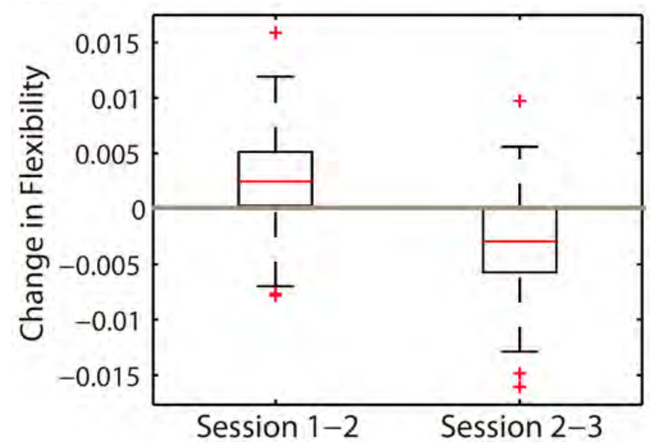

During learning, flexibility first increases and then decreases.

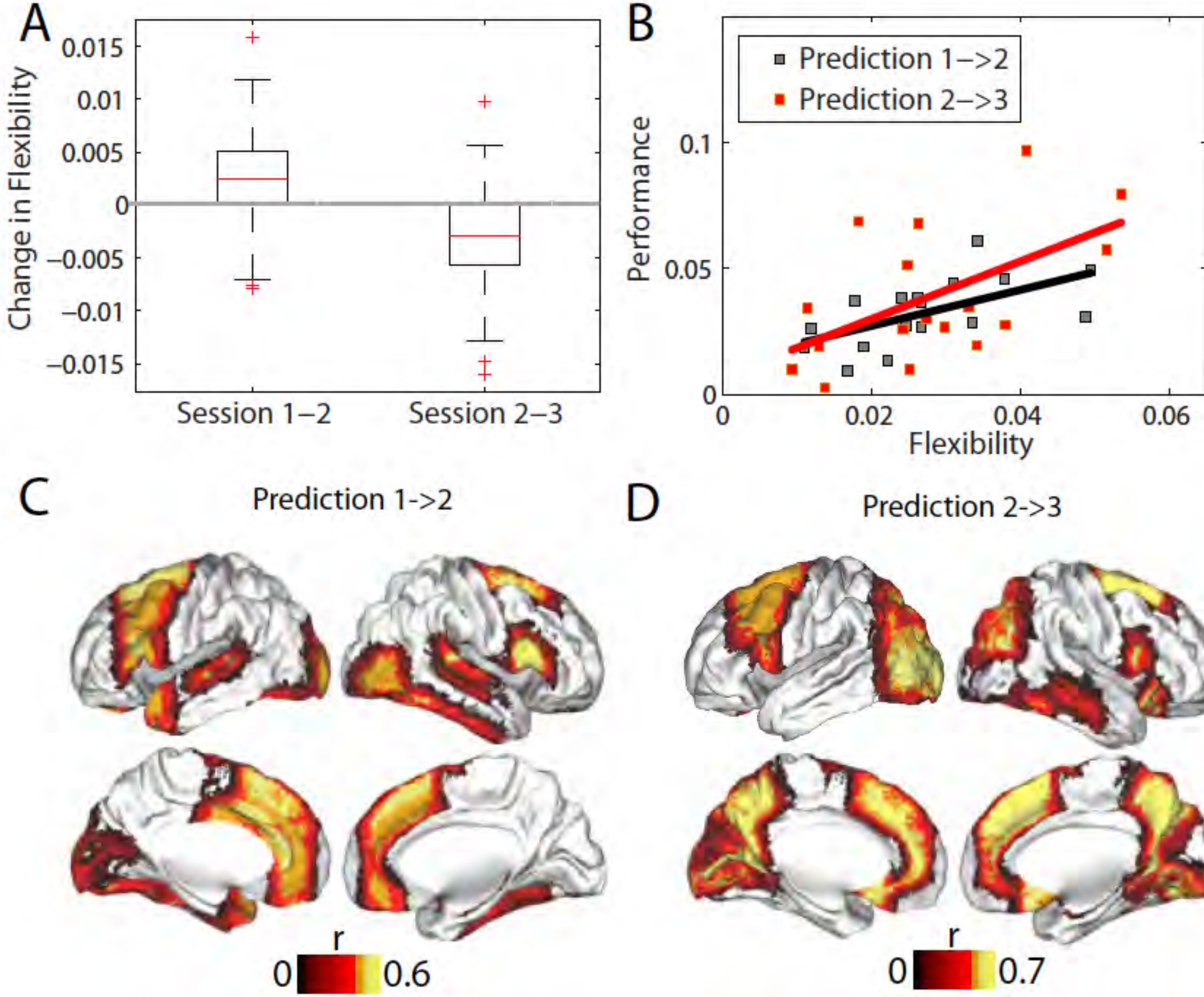

A
Change in Flexibility
0.015
0.01
0.005
0
−0.005
−0.01
−0.015
Session 1−2
Session 2−3
B
Prediction 1−>2
Prediction 2−>3
Performance
0.1
0.05
0
0.02
0.04
0.06
Flexibility
C
Prediction 1->2
D
Prediction 2->3
r
0
0.6
r
0
0.7

PEOPLE

Dani Bassett

Prof. Jean Carlson
Complex Systems
UCSB

Nick Wymbs
UCSB

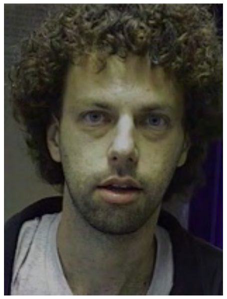

Prof. Mason Porter
Dept of Mathematics
Oxford University

Prof. Peter Mucha
Dept of Mathematics
University of North Carolina

Jesse Brown
UCLA

$$Q = \sum_{ij} [A_{ij} - P_{ij}] \delta(g_i, g_j) , \qquad (1)$$

where $\delta(g_i, g_j) = 1$ if $g_i = g_j$ and it equals 0 otherwise, and P_{ij} is the expected weight of the edge connecting node i and node j under a specified null model. (The specific choice of Q in Equation 1 is called the *network modularity* or *modularity index* [36].) A most common null model (by far) used for static network community detection is given by [33, 34, 37]

$$P_{ij} = \frac{k_i k_j}{2m} , \qquad (2)$$

where k_i is the strength of node i, k_j is the strength of node j, and $m = \frac{1}{2} \sum_{ij} A_{ij}$. The maximization of the modularity index Q gives a partition of the network into modules such that the total edge weight inside of modules is as large as possible (relative to the null model, subject to the limitations of the employed computational heuristics, as optimizing Q is NP-hard [33, 34, 38]).

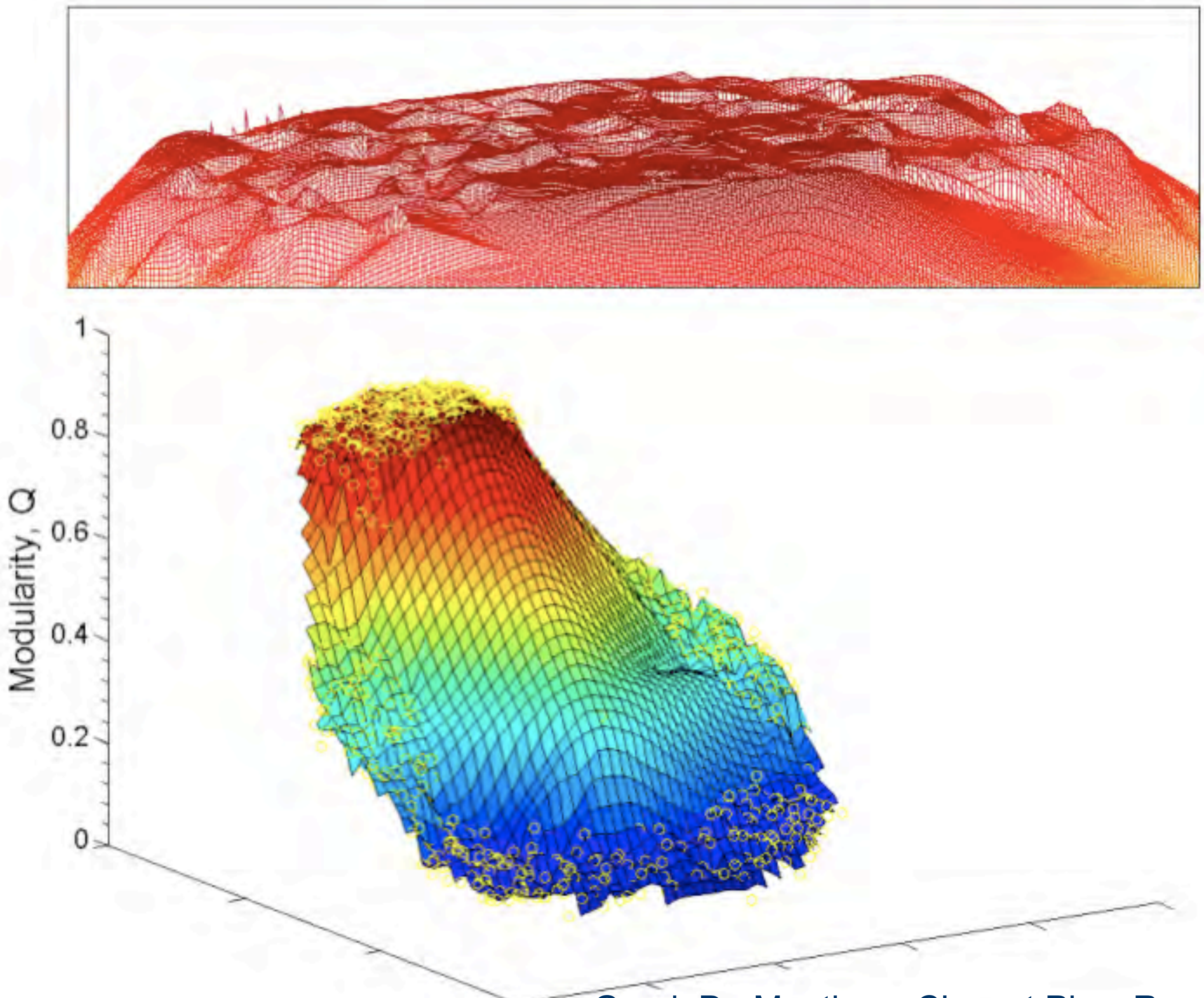

Good, De Montjoye, Clauset Phys Rev E81, 2010 multilayer networks [43].) We first defined w_{ij}^{+} to be an $N \times N$ matrix containing the positive elements of A_{ij} and w_{ij}^{-} to be an $N \times N$ matrix containing only the negative elements of A_{ij}. The quality function to be maximized is then given by

$$Q_{\pm} = \frac{1}{2w^{+} + 2w^{-}} \sum_{i} \sum_{j} \left[A_{ij} - \left(\gamma^{+} \frac{w_i^{+} w_j^{+}}{2w^{+}} - \gamma^{-} \frac{w_i^{-} w_j^{-}}{2w^{-}} \right) \right] \delta(g_i g_j) \,, \qquad (3)$$

where g_i is the community to which node i is assigned, g_j is the community to which node j is assigned, γ^{+} and γ^{-} are resolution parameters, and $w_i^{+} = \sum_j w_{ij}^{+}$, $w_i^{-} = \sum_j w_{ij}^{-}$ [42]. For simplicity, we set the resolution parameter values to unity.

Modularity in Individual Time Windows

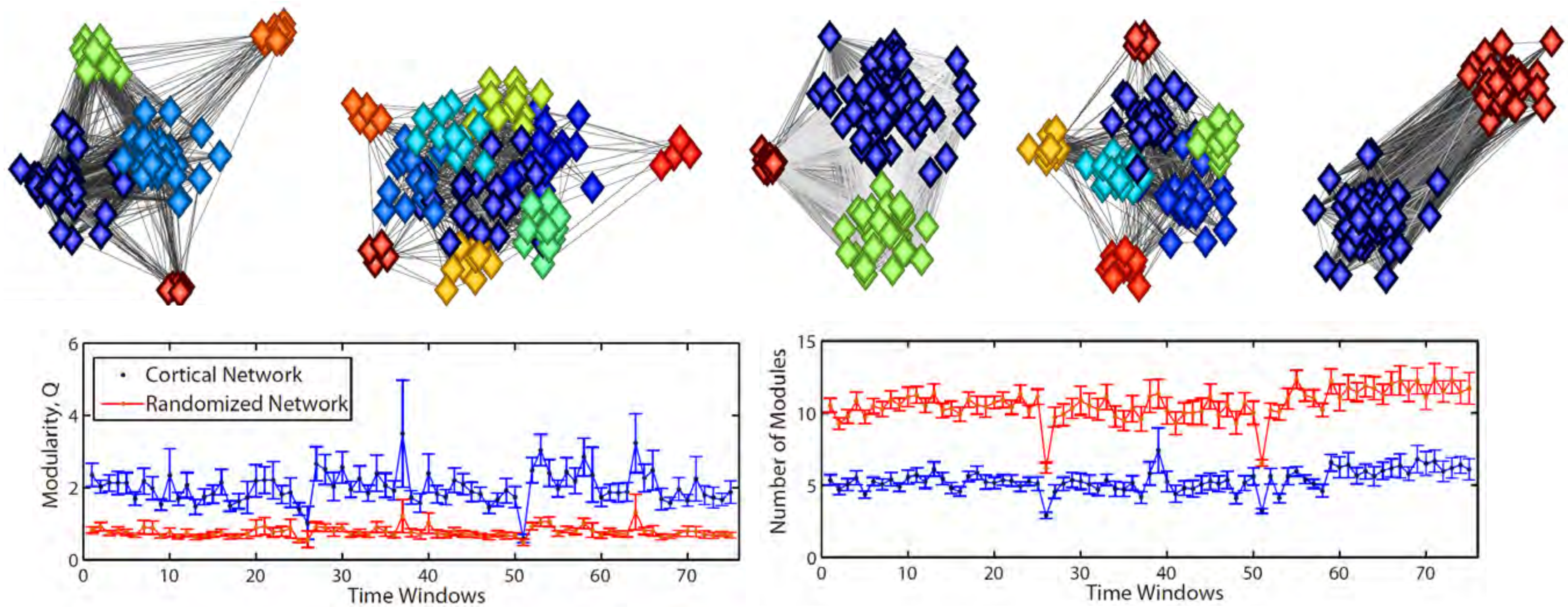

time

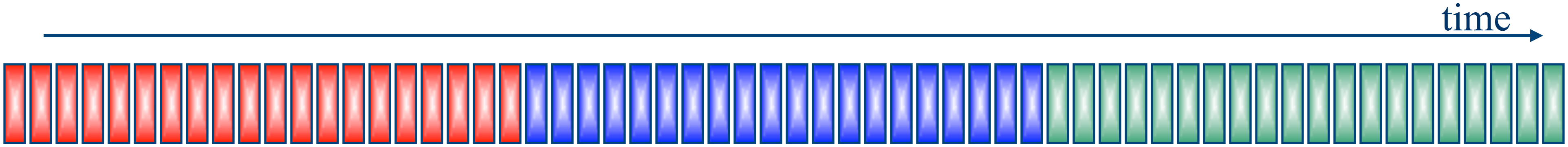

Twenty-Five Intra-Session Windows, Each ~3.45min Long

Effect of time window length on dynamic network properties

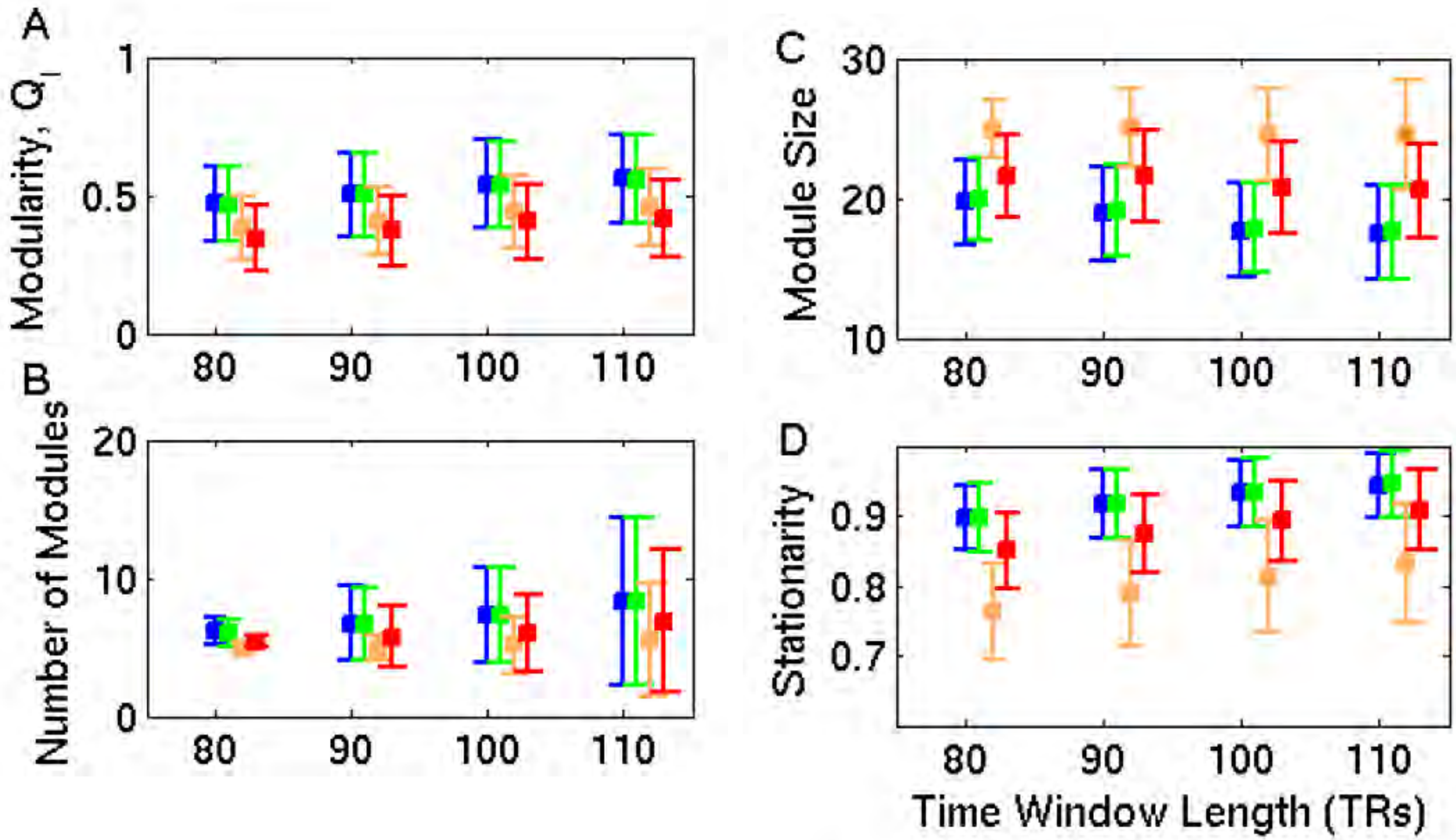

Cortical
Temporal Null
Nodal Null
Connection Null

Effect of coupling strength on dynamic network properties